12-2003

Parameter Study on Topology Optimization of Constrained Layer Damping Treatments

Rohan Vinay Pai
University of Tennessee - Knoxville

To the Graduate Council:

I am submitting herewith a thesis written by Rohan Vinay Pai entitled "Parameter Study on Topology Optimization of Constrained Layer Damping Treatments." I have examined the final electronic copy of this thesis for form and content and recommend that it be accepted in partial fulfillment of the requirements for the degree of Master of Science, with a major in Mechanical Engineering.

<div align="right">Dr._Arnold Lumsdaine, Major Professor</div>

We have read this thesis and recommend its acceptance:

Dr. J. A. M. Boulet, Dr. Frank H. Speckhart

<div align="right">Accepted for the Council:

Carolyn R. Hodges

Vice Provost and Dean of the Graduate School</div>

(Original signatures are on file with official student records.)

To the Graduate Council:

I am submitting herewith a thesis written by Rohan Vinay Pai entitled "Parameter Study on Topology Optimization of Constrained Layer Damping Treatments." I have examined the final electronic copy of this thesis for form and content and recommend that it be accepted in partial fulfillment of the requirements for the degree of Master of Science, with a major in Mechanical Engineering.

<div align="right">

Dr._Arnold Lumsdaine
Major Professor

</div>

We have read this thesis
and recommend its acceptance:

Dr. J. A. M. Boulet

Dr. Frank H. Speckhart

<div align="right">

Accepted for the Council:

___Anne Mayhew____
Vice Provost and
Dean of Graduate Studies

</div>

(Original signatures are on file with official student records)

Parameter Study on Topology Optimization of

Constrained Layer Damping Treatments

A Thesis
Presented for the
Master of Science
Degree
The University of Tennessee

Rohan Vinay Pai

December 2003

Acknowledgments

I wish to thank all those who helped me in completing my Master of Science in Mechanical Engineering. Special thanks go to Dr. Lumsdaine without his input, motivation and knowledge this work would not have been possible. He has been a great professor, mentor and advisor. I thank Dr. Boulet and Dr. Speckhart for being in my thesis committee and providing me with their valuable suggestions. I would also like to thank my family and friends for supporting me throughout this past year.

Abstract

This study investigates the optimal topology of a constrained layer damping treatment involving viscoelastic materials under a static load for different boundary conditions in order to maximize the damping loss factor for the first vibrating mode of the base structure. Different parameter studies are carried out for the two boundary conditions and conclusions are drawn based on the loss factor results and the novel topologies that emerge from these optimization results. The novel topologies are then used to interpret shapes that are more reasonable to manufacture. Tremendous improvement in the loss factor (up to 1250%) is obtained by topology optimization in many of the cases. Also this study develops fundamental understanding of the optimal topologies that are required to maximize the loss factor.

Table of Contents

List of Tables

List of Figures

Nomenclature

[M]   real mass matrix

$\{x\}$ displacement

$\{\ddot{x}\}$ acceleration

[K]   modulus matrix

$[K^i]$ complex part of the modulus matrix

$[K^r]$ real part of the modulus matrix

r   mode number

f_r eigenvalues

$\{\Phi\}_r$ eigenvectors

E_r^D dissipated energy

E_r^S strain energy

η_r damping loss factor for the rth mode

G   shear storage modulus of the viscoelastic material

υ material loss factor

E_r^V strain energy in the viscoelastic material layer in the rth mode

G'   equivalent storage modulus of the viscoelastic material

E_r^{VD} dissipated energy from the viscoelastic layer in the rth mode

E_r^{VS} strain energy in the viscoelastic layer in the rth mode

E_r^O strain energy in the elastic layer in the rth mode

ω_2 frequency at a half power point

ω_1 frequency at a half power point

ω_d damped natural frequency

$E*$ elastic modulus of the viscoelastic material

$G*$ shear modulus of the viscoelastic material

$K*$ complex bulk modulus modulus of the viscoelastic material

$\nu*$ complex Poisson Ratio

$F(\vec{x})$ objective function of design variables

$h_i(\vec{x})$ equality constraints

$g_i(\vec{x})$ inequality constraints

n   number of design variables

$d_v^{(i)}$ the fraction of viscoelastic material in element "i"

$d_e^{(i)}$ the fraction of elastic material in element "i"

f_v the total fraction of viscoelastic material

f_e the total fraction of elastic material

ρ_v density of the viscoelastic material

ρ_e density of the elastic material

E_v elastic modulus of viscoelastic material

E_e elastic modulus of elastic material

1.   INTRODUCTION

Noise and vibrations are generally regarded to be a nuisance in engineering applications. The vibrations of panels and structured members cannot be avoided when the excitation is due to shock or is random over a wide frequency range. The tendency of structures to respond vigorously to all manner of excitation is aggravated by the trends towards lightweight and unit construction with welded joints. The problems of noise and vibration are chronic in missiles, aircrafts, ships, etc., where excessive vibrations can lead to failures by fatigue. The trends towards lightweight and unit construction are giving rise to similar problems in buildings, particularly with pre-stressed concrete construction, which has very little damping.

Vibration and noise in a dynamic system can be reduced by a number of means. These can be broadly classified into active, passive and semi-active methods. Active control involves the use of certain active elements such as speakers, actuators and microprocessors to produce an 'out of phase' signal to electronically cancel the disturbance. The traditional passive control methods for air-borne noise includes the use of absorbers, barriers, mufflers, silencers, etc. For reducing structural vibration and noise, several methods are available. Sometimes just changing the system's stiffness or mass to alter the resonance frequencies can reduce the unwanted vibration as long as the excitation frequencies do not change. But in most cases, the vibrations need to be isolated or dissipated by using isolator or damping materials. In semi-active methods, active control is used to enhance the damping properties of passive elements. The full-scale implementation of active and semi-active methods is costly and complex. Passive

damping using viscoelastic materials is simpler to implement and more cost effective than semi-active and active techniques. This thesis deals with the application of viscoelastic damping materials for passive vibration and noise control, although the method used can be readily adapted to incorporate active materials.

Damping refers to the extraction of mechanical energy from a vibrating system usually by conversion into heat. Damping serves to control the steady state resonant response and to attenuate traveling waves in a structure. There are two types of damping: material damping and system damping. Material damping is the damping inherent in the material while system or structural damping includes the damping at the supports, boundaries, joints, interfaces, etc., in addition to material damping. Passive damping as a technology has been dominant in the non-commercial aerospace industry since the early 1960s (Rao, 2003). Advances in the material technology along with newer and more efficient analytical and experimental tools for modeling the dynamical behavior of materials and structures have led to many applications such as inlet guide vanes for jet engines, helicopter cabins, exhaust stacks, satellite structures, equipment panels, antenna structures, truss systems, and space stations, etc. (Rao, 2003)

When viscoelastic materials are used in vibration control, they are arranged so that they are subjected to shear or direct strains. There are two configurations, which arise as a result as shown in Figure 1.1.

- **Free Layer or Unconstrained Layer Damping Treatment**

  In this case, the damping material is either sprayed on the structure or bonded to it using a pressure sensitive adhesive. When the base structure is deflected in bending,

2

Unconstrained Layer Beam Deformed Shape

Viscoelastic Layer

Base Beam

Constrained Layer Beam Deformed Shape

Constraining Layer

Viscoelastic Layer

Base Beam
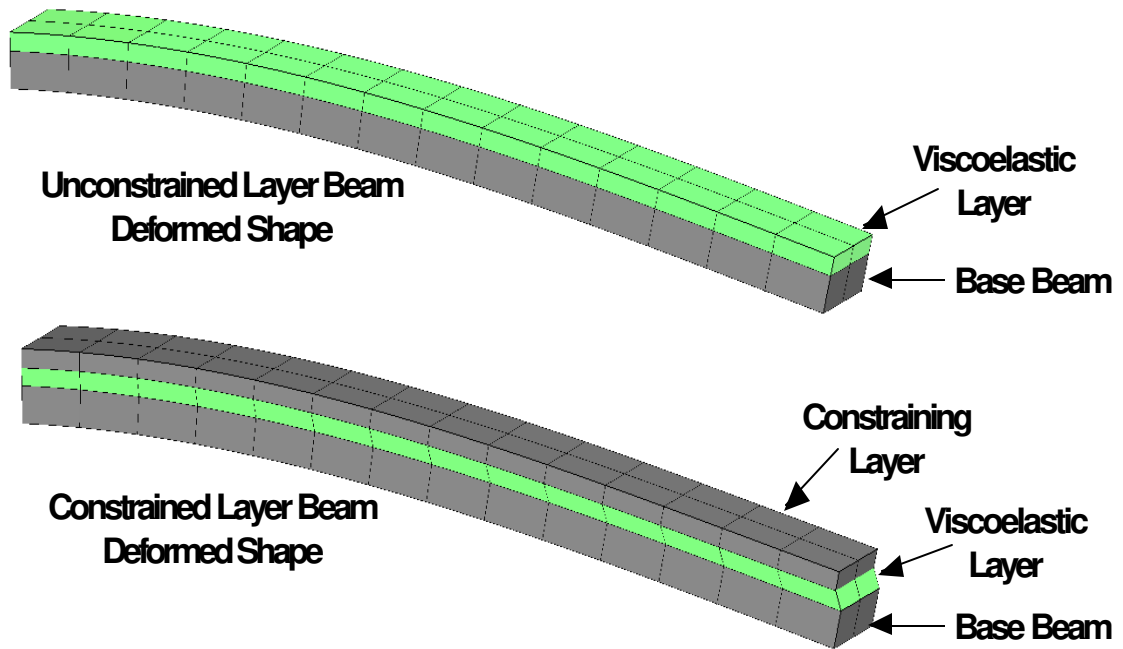
Figure 1.1 – Deformation Of Unconstrained And Constrained Layer Beams

the viscoelastic material deforms primarily in extension and compression in planes parallel to the base structure. The hysteresis loop of the cyclic stress and strain dissipates energy. The degree of damping is limited by the thickness and weight restrictions. The vibration analysis of a beam with a viscoelastic layer was first conducted by Kerwin (1959). The system loss factor of a free layer system increases with the thickness and loss factor of the viscoelastic layer.

- **Constrained Layer Damping Treatment**

  This consists of a sandwich of two outer elastic layers with a viscoelastic material as the core. When the base structure undergoes bending vibration, the viscoelastic material is forced to deform in shear because of the upper stiff layer. The constrained layer damping is more effective than the free layer design since more energy is consumed and dissipated into heat in the work done by the shearing mode in the viscoelastic layer. Damping tape consists of a thin metal foil covered with a viscoelastic adhesive and is used on an existing structure in a constrained layer arrangement.

Although these designs have been around for over 40 years, recent improvements in the understanding and application of the damping principles, together with advances in materials science and manufacturing, have led to many successful applications. The key point in any design is to recognize that the damping material must be applied in such a way that it is significantly strained whenever the structure is deformed in the vibration mode under investigation.

The aim of this research is to determine the optimal topologies for viscoelastic laminae used for vibration damping in order to maximize the damping loss factor of the structure. The robustness of the topology optimization method presented will be examined by varying certain parameters and determining the effect on the optimal topology and the damping levels achieved.

1.1 LITERATURE SURVEY

One of the first analytical studies of unconstrained layer beams was conducted by Oberst and Frankenfeld (1952). Commonly used methods for analysis of unconstrained and constrained damped laminated structures were developed by Ross, Ungar, and Kerwin (1959). This work led to numerous studies, some of which are reviewed by Nakra, (1976, 1981, and 1984). Finite elements have commonly been employed to characterize the laminated structure (for example, Hwang, Gibson, and Singh, 1992). Recently, constrained damping layers have proven effective for vibration damping in microstructures (Hsu and Shen, 2002). A review of recent industrial applications of these materials is given by Rao (2003).

The desire to apportion this material in a way that will take the greatest advantage of its dissipative characteristics has led to studies in optimization. Lundén (1979 and 1980) examined optimal designs of constrained damping layers for both beam and frame structures. Plunkett and Lee (1970) optimized constraining layer tape lengths on beams in order to maximize the system loss factor. Lekszycki and Olhoff (1981) optimized the

shape of an unconstrained damping layer for a beam structure using variational techniques. Lall, et al (1983) maximized the system loss factor of damped sandwich panels (symmetric constrained layer plates) including the frequency dependence of the viscoelastic materials. They also demonstrated that minimizing the peak displacement produces different results than maximizing the system loss factor. Lifshitz and Leibowitz (1987) maximized the system loss factor, modeling a sandwich beam using a sixth order constrained layer theory. Lin and Scott (1987) optimized the shape of a damping layer for both constrained and unconstrained beams, using structural finite elements to model the structure. Hajela and Lin (1991) used a global optimization strategy to maximize the system loss factor with respect to damping layer lengths for a constrained layer beam. Studies have also been performed in the optimal design of unconstrained damped laminated plate structures. Yildiz and Stevens (1985) optimized the shape of an unconstrained plate damping layer. Roy and Ganesan thoroughly examined possible partial damping layer treatments for plate (1993) and beam (1996) unconstrained damping layers. Lumsdaine and Scott (1995) optimized the shape of a symmetric unconstrained damping layer for both beams and plates using structural finite elements for modeling. They also examined how the optimal shape is affected depending on whether the viscoelastic material is assumed to have constant or frequency varying viscoelastic properties. Lumsdaine and Scott determined the optimal shape for unconstrained (1998) and constrained (1996) damping layers using continuum finite elements for modeling. Liu and Chattopadhyay (2000) optimized segmented constrained damping layers to improve helicopter aeromechanical stability. All of these studies performed shape or size optimization assuming a certain topology for the laminate.

6

Topology optimization is a relatively recent field and has been shown to be a good method for finding optimal topologies for structural problems with given boundary conditions. Bendsøe and Kikuchi (1988) first introduced the homogenization method for finding the optimal topology for a structural problem. A more thorough description of topology optimization using homogenization is given in the books by Hassani and Hinton (1999), Allaire (2002) and Bendsøe and Sigmund (2003).

Topology optimization using the homogenization method has recently been used to maximize the damping characteristics of a viscoelastic material (Yi, et al, 2000), but not in the context of a constrained layer-damping problem. Van der Sluis, et al (1999) have performed topology optimization of heterogeneous polymers using homogenization. But that study was purely static, and did not examine damping properties. Three-phase composites have been studied recently in the context of optimizing thermal expansion for a composite (Sigmund and Torquato, 1997), but not in the context of a passive constrained damping layer.

In a previous work (Lumsdaine, 2002) a constrained damping layer topology was optimized. The results presented in this thesis are an extension of that work. The volume of damping material and constraining layer material are varied, as is the thickness of the base beam structure. Additionally, a more accurate method is used to compute the system loss factor.

1.2   PROBLEM STATEMENT

The objective of this study is to determine the best two dimensional topology of a damping treatment so as to maximize the loss factor for the first resonance frequency. The beam used for this study is a three-layered beam consisting of a base elastic structure, a soft viscoelastic layer and a stiff elastic layer on top of it. The topology of the base structure remains unchanged while that of the other two layers is allowed to change according to the optimization objective of maximizing the loss factor at the first bending mode. To determine the best topology, a numerical optimization is conducted. Finite elements are typically used for topology optimization problems, as analytical formulations would be far too complex to use practically. Thus, the beam is modeled using finite elements with two-dimensional first-order plane stress continuum elements. Analysis is done using the commercial finite element code ABAQUS. The loss factor is computed using the modified modal strain energy method (Xu, et al, 2002) in the optimization process. For the initial and optimal topologies, the loss factor results are validated by using the half-power bandwidth method. A commercial code is used for the optimization, which uses an SQP (sequential quadratic programming) algorithm. For details on the algorithm and the code used (NLPQL), see Schittkowski (1986).

Several different studies were performed for this work. The volume of damping material and constraining layer material, i.e. material fraction, is varied, as is the thickness of the base beam structure. This parameter study is carried out for two different boundary conditions, i.e. simply supported beam and a cantilever beam.

Also, a few manufacturable solutions are discussed based on the novel topologies that emerge from the resulting configurations.

Chapter two gives an overview of the finite element modeling, the modal strain energy method and related theory on which the problem is based. Chapter three explains the basic idea of optimization and gives a detailed description of topology optimization. The implementation of the finite element model in the optimization algorithm is described. Chapter four shows the results of the parameter study for different optimizations. Also included in this chapter are the configurations, which are more reasonable to manufacture, that emerge from the resultant topologies. The last chapter shows the conclusions of this work and gives an overview of possible future work.

2.   ANALYTICAL AND NUMERICAL FORMULATIONS

Viscoelastic composites have been widely applied for the purpose of reducing noise and vibration. These long chain molecule polymers can be used with advantage because their imperfect elasticity gives much larger energy dissipation when deformed compared with metals. They therefore possess the desirable damping characteristics and provide design flexibility, i.e., tradeoff between damping and stiffness.

Viscoelasticity may be defined as material response that exhibits characteristics of both a viscous fluid and an elastic solid. An elastic material such as a spring retracts to its original position when stretched and released, whereas a viscous fluid such as putty retains its extended shape when pulled. A viscoelastic material combines these two properties, i.e., it returns to its original shape after being stressed and released, but does it slowly enough to oppose the next cycle of vibration. The degree to which a material behaves either viscously or elastically depends mainly on temperature and the rate of loading (frequency in a steady state case).

Examples of viscoelastic materials are: polymeric materials such as plastics, rubbers, acrylics, silicones, vinyls, adhesives, urethanes, epoxies, etc. The degree of viscoelasticity is measured by the ratio of the real part of the bulk modulus to the complex part.

This chapter gives an overview of the modal strain energy method with its assumptions and modifications involved as well as the modeling of the structure to be studied using a commercial finite element software package.

To analyze the dynamic performance of the damping treatments, considerable effort has been devoted to the studies of dynamic characteristics of viscoelastically damped structures (Nashif, et al, 1985). There are two major approaches in the analysis of damping effect: analytical and numerical .

The analytical approach is usually applicable to relatively simple structures, such as sandwich beams and plates, etc. The earliest analytical work on damping analysis can be found mostly related to the viscoelastic material property characterization. To develop an understanding of the parameters in the constrained layer damper, Ross, Kerwin and Ungar (1959) outlined the dominant design parameters for the case where all layers vibrate with the same sinusoidal spatial dependence. The outer layers are assumed to deform as Euler-Bernoulli beams and the viscoelastic layer is assumed to deform only in shear, which leads to a single fourth order beam equation where the equivalent complex bending stiffness depends on the properties of the three layers. Di Taranto (1965) studied damped sandwich beams with arbitrary boundary conditions. He derived a sixth-order differential equation of motion for the beam and assigned a complex shear modulus to the sandwiched core. To extend Ross, Kerwin and Ungar's analysis to beams with general boundary conditions in which sinusoidal spatial dependence cannot be assumed, Mead, et al., (1969) obtained a sixth order equation of motion. It is assumed that the beam's deflection is small and uniform across a section, the axial displacements are continuous, the base and constraining layers bend according to the Euler hypothesis, the damping layer deforms only in shear, and the longitudinal and rotary inertia effects are insignificant. The validity of the analysis is therefore limited to some upper range of core stiffness. Miles, et al, (1986) obtained a sixth order equation of motion by using

Hamilton's principle. The assumptions were equivalent to those of Mead except that relative transverse deflection is permitted between the outer layers and longitudinal inertia is included.

Though analytical methods are useful for predicting damping characteristics of some simple structures, a numerical approach, mainly the finite element method, remains to be the method of choice when complex physical systems are analyzed. In the finite element analysis of structures with viscoelastic damping material treatment, there are two issues making the analysis a difficult task. One is that although the modulus of a viscoelastic material is normally complex in steady state harmonic analysis, most commercial finite element packages are not designed to deal with complex modulus efficiently and accurately. The other one is that the material properties of viscoelastic material are frequency dependent, which creates a non-linear eigenvalue problem for the dynamic analysis. To deal with the complex modulus of the viscoelastic material, several different techniques have been developed, of which modal strain energy method has become a commonly used approach. In the modal strain energy method, the structure is first assumed to be undamped and modeled using the real part of the complex modulus as modulus of the damping layer. The real eigenvectors of each mode are obtained from finite element analysis and strain energies in all layers of the structure are calculated. The dissipative energy of the structure is calculated proportional to the strain energy in the damping layer and the material loss factor, and the modal loss factor is obtained by calculating the ratio of the dissipative energy to the total structural energy. However, modal strain energy method becomes quite inaccurate when the damping of the structure becomes high. Additionally, it is difficult to include properties that vary with frequency

or temperature. To consider the frequency and temperature dependence of elastic modulus of viscoelastic material, an iterative method is normally combined with commercial finite element software. This requires a significant amount of computational effort since for each mode, eigen-solutions need to be repeated until converged results are obtained.

2.1   THE MODAL STRAIN ENERGY METHOD

When a structure with viscoelastic damping treatment is to be analyzed, finite element modeling procedure can be used to establish its mass matrix [M], and stiffness matrix [K]. The structural eigenvalue problem can be written as,

$$[M]\{\ddot{x}\} + [K]\{x\} = 0 \dots\dots\dots\dots\dots\dots\dots\dots(1)$$

where [M] is a real matrix and

$$[K] = [K^r] + i[K^i]$$

is a complex matrix due to the complex modulus of the viscoelastic damping material used in the structure.

However, there are two main issues associated with the eigen-problem of (1). One is that most commercial finite element software does not have the corresponding solver for the complex eigen-solution for a damped structure. Another one is that the modulus and loss factor of the viscoelastic material are frequency / temperature dependent, which results in the eigen-problem of (1) being non-linear.

13

The modal strain energy method is one of the most economical approaches in dealing with the complex modulus of the damping material. It assumes that the damped structure has the same natural frequencies and modal shapes as the undamped structure, thus the eigen-problem of the undamped structure is written as,

$$[M]\{\ddot{x}\} + [K^r]\{x\} = 0 \dots\dots\dots\dots\dots\dots\dots(2)$$

By solving (2), eigenvalues and eigenvectors,

$$f_r, \{\Phi\}_r$$

r = 1,2,3,…can be obtained.

For the rth mode, the dissipated and strain energies are defined as :

$$E_r^D = \{\Phi\}_r^T [K^i]\{\Phi\}_r$$
$$E_r^S = \{\Phi\}_r^T [K^r]\{\Phi\}_r$$

The damping loss factor for the rth mode, η_r, therefore becomes,

$$\eta_r = \text{energy lost per cycle / energy stored per cycle}$$

$$\eta_r = \frac{E_r^D}{E_r^S} = \frac{\{\Phi\}_r^T [K^i]\{\Phi\}_r}{\{\Phi\}_r^T [K^r]\{\Phi\}_r}$$

Since the complex modulus can be expressed as $(1 + i\upsilon)G$, where G is the shear storage modulus of the viscoelastic material, and υ is the material loss factor, and in finite element analysis, the strain energy in the viscoelastic material layer, E_r^V, can be also calculated, thus the damping loss factor of the rth mode can be estimated (Refer ANSYS Theory Manual 5.5) as,

$$\eta_r = \frac{\upsilon_r E_r^V}{E_r^S}$$

where υ_r is the material loss factor at the natural frequency of the rth mode. Xu, et al, (2000) compared the result for a cantilever sandwich beam using the above mentioned modal strain energy method with that from direct complex eigen-solution using compound beam element, and found that the results from both methods are very close when the material loss factor is low, however, significantly different when the material loss factor becomes high.

However, due to viscoelastic materials' frequency dependent feature of the storage shear modulus G and loss factor η, the structural stiffness matrix in (1) is not only a complex one, but also in theory a function of frequency. Therefore, the dynamic characterization of a damped structure is not completely modeled by a single application of the modal strain energy method as outlined above. The storage shear modulus G and loss factor η of viscoelastic material are also temperature dependent. However, that is not going to be considered here since in most dynamic analysis, constant temperature could be assumed.

Then the $[K^r]$ in (2) varies with the frequency of the in question mode. The modal analysis of the non-linear eigen-problem can be normally simplified to an iterative process. For the modal parameters f_r, η_r, and $\{\phi\}_r$ of the rth mode, the method can be summarized as,

Initialize: $f = f_0$, find the corresponding $G = G (f_0)$, and calculate $[K^r] = [K^r (f_0)]$

For k = 1,2,3,...

Solve (2) $\rightarrow$ $f_r^{(k)}$, $\eta_r^{(k)}$, *and* $\{\phi\}_r^{(k)}$

If $\left| f - f_r^{(k)} \right| / f_r^{(k)} \le \varepsilon \rightarrow STOP$

Update: $f = f_r^{(k)}$, *find the corresponding* $G = G(f_r^{(k)})$ *and calculate* $[K^r] = [K^r(f_r^{(k)})]$

As the iteration continues, the estimated $f_r^{(k)}$, $\eta_r^{(k)}$, and $\{\phi\}_r^{(k)}$ will converge at the exact solution f_r, η_r, and $\{\phi\}_r$. Similarly, modal parameters of other modes can be determined. This iterative process requires a significant amount of computational effort. Especially in the process of viscoelastic material selection, the process needs to be repeated for each material trial. Hence, we have not used this process in the research. But the assumption that the viscoelastic properties are frequency independent holds true in our case since we are considering a very small frequency range. The inaccuracies, if any, are worth the gain in computational time.

2.2   THE REVISED MODAL STRAIN ENERGY METHOD

The revised modal strain energy method was developed by (Xu, et al, 2002). As mentioned above, the traditional modal strain energy method uses the real eigenvector of each mode obtained from finite element analysis of the corresponding undamped

structure to calculate strain energy in each material layer. The dissipative energy is calculated proportional to the strain energy in the viscoelastic damping material layer and the material loss factor. The modal loss factor is then obtained by calculating the ratio of the dissipative energy to the total structural strain energy. The problem associated with this approach is that the errors in natural frequency and modal loss factors estimation increase dramatically when the material loss factor increases. The reason is that the traditional modal strain energy method uses the real part of the material modulus in the finite element analysis such that the natural frequencies do not change with material loss factor. Hence a revised modal strain energy method is discussed here.

In order to consider the effect of material loss factor on the structural natural frequencies, it is suggested to use an equivalent modulus, the magnitude of the viscoelastic material modulus, i.e. $G' = G*\sqrt{(1 + \upsilon^2)}$, instead of G, in the undamped structural modal analysis, and use the resulting frequencies as the ones of the damped structure. When the equivalent modulus is used, the natural frequencies of the structure will increase with the loss factor even when the storage modulus of the viscoelastic material remains the same, which agrees with results obtained by direct complex eigen-solution.

After the modal analysis of the equivalent undamped system is completed, the strain energies in different materials can be calculated accordingly. To estimate the modal loss factor, the strain energy and the dissipative energy in the viscoelastic material need to be obtained as follows:

$$E_r^{VS} = \frac{1}{\sqrt{1+\upsilon^2}} E_r^V$$

$$E_r^{VD} = \frac{\upsilon}{\sqrt{1+\upsilon^2}} E_r^V$$

where, E_r^V is the total strain energy of the rth mode in the viscoelastic material by assuming the modulus to be G'. If the strain energy in all other materials is E_r^O, then the modal loss factor of the rth mode can be estimated by,

$$\eta_r = \frac{E_r^{VD}}{E_r^O + E_r^{VS}} = \frac{\upsilon_r E_r^V}{E_r^O \sqrt{1 + \upsilon_r^2} + E_r^V}, \quad r = 1,2,3,\ldots$$

It is obvious that the simplified process requires only a limited number of structural FEM analysis, so it can avoid the significant amount of computational effort that would be required. Hence, the modified modal strain energy method has been used to calculate the modal loss factor of the composite structure used in this research.

2.3   MODELING

Using the modified modal strain energy method described above, the system loss factor at a given mode may be estimated from the undamped mode shapes of the laminated structure and the material loss factor of the viscoelastic material. Its implementation with a commercial finite element software package was given by Johnson and Kienholz (1982). The system loss factor may also be defined by the half-

power bandwidth method as shown in Figure 2.1, which requires obtaining the forced

response over a wide frequency range (see Ewins, 2000):

$$\eta = \frac{\omega_2{}^2 - \omega_1{}^2}{2\omega_d{}^2}$$

where ω_1 and ω_2 are the frequencies at the half power points and ω_d is the damped natural

frequency. In cases where the damping is light, this equation reduces to:

$$\eta = (\omega_2 - \omega_1)/\omega_d$$

which is the familiar form of the system loss factor. The system loss factor will be

calculated and used for monitoring the improvement in damping performance for the

optimal designs.

It is not necessary to include viscoelasticity in the material modeling for the FE

analysis when using the modal strain energy (MSE) method, as it uses the modes

computed from the purely elastic equivalents of the material constituents. Since results

obtained using the MSE method are obtained by an eigenvalue extraction of the

undamped modes, it is much less computationally intensive than the half-power

bandwidth method, which is an exact method and requires finding the forced response of

the damped system over a wide frequency range.

However, the loss factor results obtained using the MSE method are confirmed

using the half-power bandwidth method, in which case it is necessary to accurately model
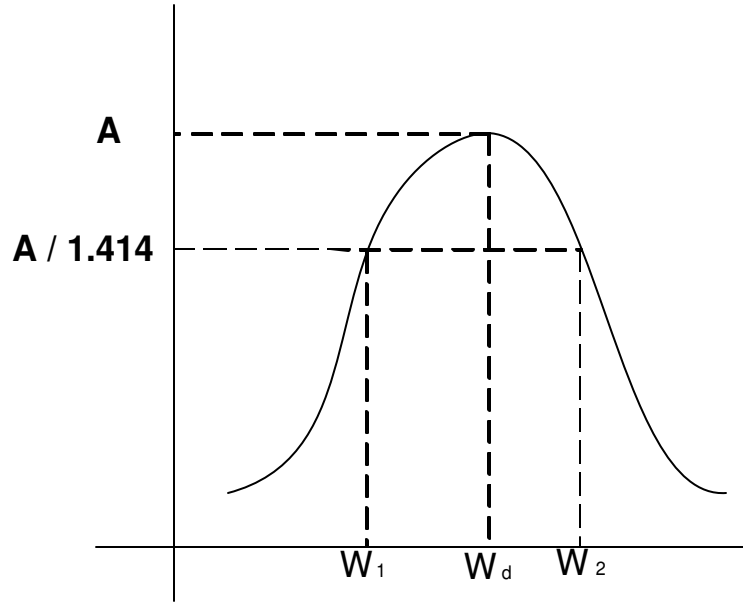
viscoelasticity.

Figure 2.1   Half Power Bandwidth Method

Lumsdaine and Scott (1998) did a shape optimization of unconstrained viscoelastic layers using continuum elements. In it, the viscoelastic properties were modeled as follows. For a linear isotropic viscoelastic material, the elastic modulus and shear modulus may be written as,

$$E^* = E_1 + iE_2$$

$$G^* = G_1 + iG_2$$

The above equation can also be written as,

$$G^* = G_1[1 + i\upsilon_m]$$

Here E_1, E_2, G_1 and G_2 denote the storage and loss moduli for extension and shear, respectively, and υ_m is the material loss factor. In the sequel, the frequency dependence of these and other material properties will not be explicitly noted. The complex bulk modulus is given by,

$$K^* = K_1 + iK_2 = E^* / 3(1 - 2\nu^*)$$

where "ν^*" is the complex Poisson ratio defined through

$$G^* = E^* / 2(1 + \nu^*)$$

Viscoelastic properties can be entered into ABAQUS in several ways. In the frequency domain, tabular values of G_1, G_2, K_1, and K_2, suitably normalized, can be entered as functions of frequency. The dynamic elastic modulus and Poisson's ratio may be related to the dynamic shear modulus and bulk modulus in the same way that the

equivalent static properties are related. Thus a dynamically varying Poisson ratio may be taken into account in entering the shear and bulk moduli.

Very little Poisson's ratio data is available for viscoelastic materials in general. Often, viscoelastic materials are assumed to be incompressible ($\nu = 0.5$) in regions of rubbery behavior (low frequencies / high temperatures), and to have a Poisson's ratio of about 0.33 in regions of glassy behavior (high frequencies / low temperatures). The fact that Poisson's ratio varies with frequency, temperature, and strain magnitude is well documented (see Rigbi, 1967 and Moran and Knauss, 1992). The measurement of this variation is very difficult to obtain experimentally, however, and is not available for most damping materials. The operating frequencies examined are around 100 Hz, which is in the damping material's transition region. In the absence of any specific data for this material, a constant Poisson's ratio of 0.4 (between 0.33 and 0.5) is assumed.

The structure analyzed in this study is modeled with two-dimensional plane stress continuum elements. The commercial finite element code ABAQUS is used for the structural modeling. Eight-noded quadratic elements are used for modeling. These elements are used because of their higher aspect ratio modeling capability. These can have an aspect ratio as high as 100, which allows us to use fewer elements and thus fewer design variables.

Aluminum is used as the elastic material for the base layer and the constraining layer. The damping material is a commercially available ISD 112 from 3M. Material properties used in this study are listed in Table 2.1 below. Properties for the damping material are taken at 100 Hz and 20 degrees Celsius. The material loss factor is 1.0.

TABLE 2.1 – Material Properties

	Aluminum	Damping Material
Density	2710 kg/m^3	1100 kg/m^3
Elastic Modulus	68.9 GPa	2.8 MPa
Poisson's Ratio	0.35	0.4

Properties are assumed to be frequency invariant. This assumption should not result in substantial inaccuracies, as all the simply supported structures studied have natural frequencies between 95 and 125 Hz and the cantilever structures studied have natural frequencies between 35 Hz to 55 Hz. Future studies could include frequency dependence using the Golla-Hughes-McTavish method (such as Lam, et al., 2000) or augmenting thermodynamic fields (see Lesieutre and Mingori, 1990).

The base aluminum beam in this study is subjected to the two different boundary conditions for which the parameter study is carried out i.e. a simply supported beam and a cantilever beam. It is 150 millimeters long and 1 millimeter high. Only half of the beam in modeled in view of symmetry for the simply supported case. But for the cantilever case, the full beam needs to be modeled. The design space for the constrained damping layer is 0.5 millimeters high, with sixteen elements across the length (9.375 millimeters per element) and five elements through the thickness (0.1 millimeters per element), as shown below in Figure 2.2. Hence, the aspect ratio of each element is 93.75. The limit of accuracy for the aspect ratio is 100. Hence we have sufficient accuracy. These dimensions are typical of commercially available constrained damping layers.

Figure 2.2 shows a sample initial configuration of the 20% material fraction case. The elastic base beam is shown without any elements for clarity. The viscoelastic material is shown by the green elements and the constraining layer elastic material is shown by the black elements. The three layers of 16 elements each on top of these two layers, which are also shown, do not contain any material initially and are void, but they are part of the design space used for optimization. This configuration is the starting point of the optimization process. Some material might be placed in these spaces,

Figure 2.2   Sample Initial Configuration For The 20% Case

which start as void initially, after the optimization run has been completed. Though the base beam and the stiff elastic constraining layer are made up of essentially the same material, the figure represents them by two different colors for clarity, since only the constraining layer is part of the design space from the view point of optimization. The topology of the base beam remains unchanged. Each location has 2 elements and each element can take either of the two densities, i.e. elastic or viscoelastic or a combination of the two.

3. TOPOLOGY OPTIMIZATION

Over the past fifteen years, structural topology optimization research has experienced considerable progress. Simply stated, topology optimization consists of determining the best arrangement of a limited volume of structural material within a given spatial domain so as to obtain the optimal mechanical performance of the concept design. The optimization process systematically and iteratively eliminates and re-distributes material throughout the domain to obtain a concept structure. An attractive aspect of continuum structural topology optimization is that it can be applied to the design of both materials and structural systems or elements. The development of new methods in structural topology optimization and investigating the characteristics and applicability of these methods in the design of large-scale civil-structural systems, small-scale flexible mechanisms, e.g. MEMS, and intermediate-scale mechanical systems, as well as in the arrangement of composite materials for specific performance characteristics is being pursued currently.

Initially, the available material is evenly distributed throughout the design space. In many cases, there is also a random distribution. The material is then iteratively re-distributed within the design space in order to minimize compliance. The resulting material layout provides the optimal starting point for the design.

3.1 OPTIMIZATION

The concept of optimization is a basic idea in engineering. The desire to improve design, for example to make products better, lighter, cheaper or more reliable, has been a major idea since early engineering years. Numerical optimization has been proven to be a useful tool for improving complex designs. This chapter gives an overview of the general idea of optimization routines used and how the optimization problem is stated for the given case.

3.2 INTRODUCTION

In general, an optimization problem begins with a set of independent design variables and usually includes conditions or restrictions that define acceptable values for these variables (constraints). For given values of design variables it must be possible to compute an objective function, which gives a measure for the "goodness" of the design. In mathematical terms, optimization is the minimization or maximization of an objective function within given constraints on the design variables. The general form of an optimization problem can be expressed in mathematical terms as:

$$\min_{x \in R^n} F(\vec{x})$$

subject to $\qquad h_i(\vec{x}) = 0, \qquad i = 1, 2, \ldots, m$

$$g_i(\vec{x}) \leq 0, \qquad i = 1, 2, \ldots, l$$

where the objective and constraint functions are continuous real-valued scalar functions.

3.3   HOMOGENIZATION

The traditional way of finding the best shape or topology for a mechanical structure is an iterative trial-and-error approach. The design engineer uses his experience and intuition to find a solution to a given problem. Mechanical or numerical tests then show if the design meets the specified criteria. If the design fails, the design engineer enhances the design until a satisfying result is found. This system requires both special skill and experience for a truly good design and it does not guarantee that the best possible design has been found.

Structural topology optimization can be thought of as determination of the optimal spatial material distribution. In other words, for a given set of loads and boundary conditions, the material is redistributed in order to minimize the objective. Therefore, the general shape optimization problem can be considered as a point-wise material/no-material approach. However, implementation of this on-off approach to an optimization problem requires the use of discrete optimization algorithms. Such approaches have been shown to be time consuming and unstable, unless materials with composite microstructure are introduced (Hassani and Hinton 1999). Considering a composite consisting of an infinite number of small holes, which are periodically distributed, can solve this problem (Figure 3.1). In fact, using a cellular body with a periodic microstructure moves the on-off approach of the problem from the macroscopic scale to
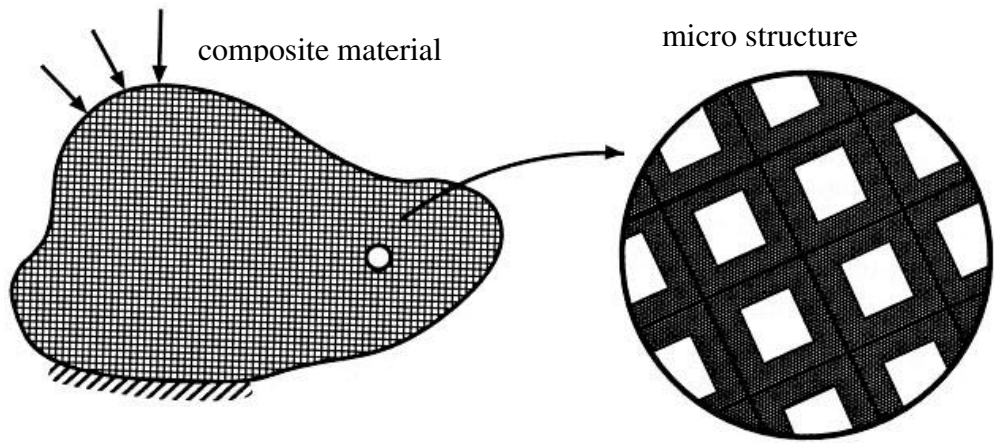
FIGURE 3.1 - Homogenization Through Micro Cells With Rectangular Holes (Hassani And Hinton 1999)

the microscopic scale (Bendsoe 1988). One approach to introduce these microstructures is homogenization. The theory of homogenization is used to determine the macroscopic mechanical properties of these materials. In practice, after choosing the design domain and the finite element discretization, it is assumed that each element consists of a cellular material with a specific microstructure. The geometrical parameters of these microstructures are the design variables of the optimization problem. In the simplest case the microstructure has rectangular holes or voids (as shown in Figure 3.1) and the mechanical properties become proportional to the density of the material.

Figure 3.2 illustrates this process for the design of a bracket using homogenization, where the design domain and the boundary conditions are shown in Figure 3.2(a). The optimization process varies the density of each finite element, which is shown through a gray scale in the picture. A cell that is completely black corresponds to a density of 100%, where as a cell that is completely white corresponds to a density of 0%. The optimal material distribution for this problem (a stiff lightweight design) is shown in Figure 3.2(b). Since materials with intermediate densities are artificial difficult to manufacture, this solution needs to be interpreted. This is done in Figure 3.2(c). Furthermore, general manufacturing rules can be applied, which leads to the final solution of this problem, shown in figure 3.2(d).

3.4   OPTIMIZATION METHODOLOGY

Several approaches are possible for optimizing the topology of constrained layer damping structures. The problem could be posed as a discrete optimization problem,
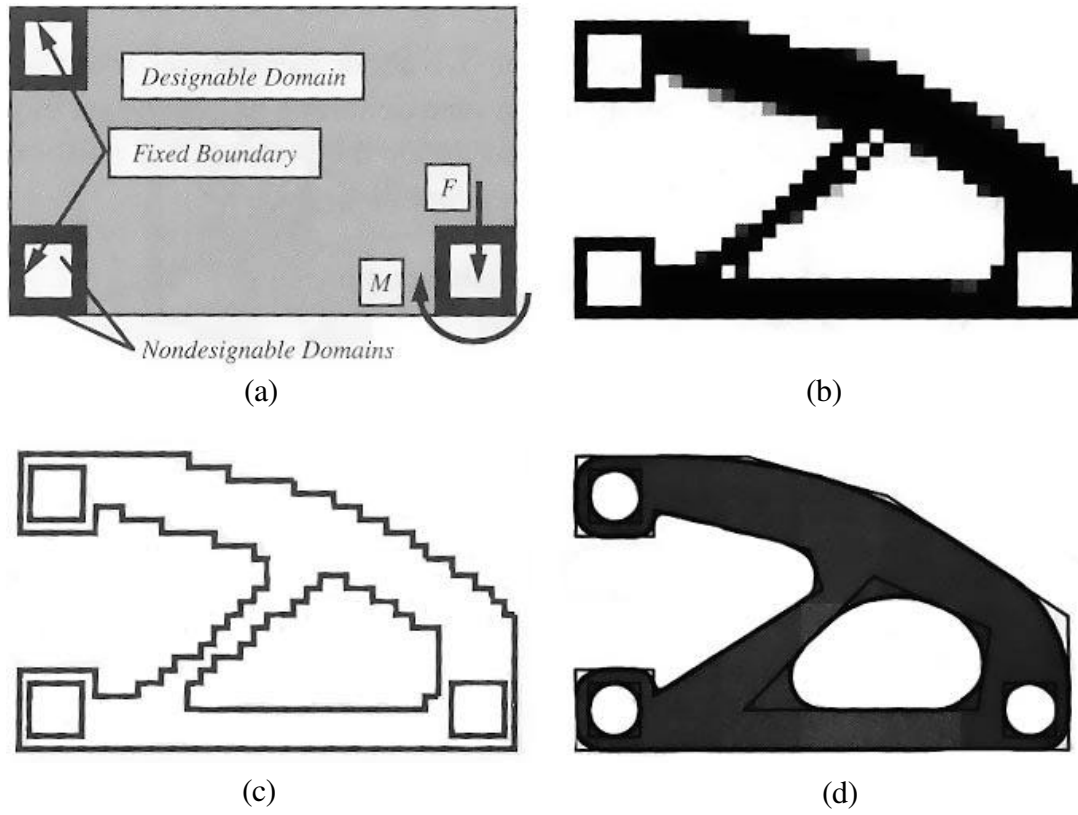
In figure (a): Designable Domain, Fixed Boundary, Nondesignable Domains, F, M

(a) (b) (c) (d)

FIGURE 3.2 - Optimal Topology Design (Papalambros And Douglas 2000)

where each element is either viscoelastic material, elastic material or empty. This would require the use of a global optimization algorithm (such as simulated annealing or a genetic algorithm). This approach has two shortcomings. First, the computational requirements for a mesh of reasonable density would be prohibitive. Second, it has been shown that the problem posed as such lacks a mathematical solution (Bendsoe, 1995). The practical drawback that results from this mathematical shortcoming is that the optimal result is sensitive to the finite element mesh discretization. Another approach is to allow the material properties of each element to vary, making the design variables continuous. The homogenization method has been commonly used to accomplish this (see Bendsoe and Kikuchi, 1998 for the seminal work on the use of homogenization in structural optimization). Many studies in topology optimization have effectively used less rigorous approaches to topology optimization (for example, Yang and Chuang, 1994, and Rozvany, et al, 1992).

Figure 3.3 shows the symmetric finite element model used for topology optimization in this research. It consists of a base beam and the constraining layers on top of it divided into 5 layers of 8 elements each for the simply supported case. The exploded view of just one column of elements is shown.

In this research, a simple material model is used, where the normalized density and modulus of the material for each element are allowed to vary together from 0% (in actuality, not zero but a very small value in order to prevent singularities in the stiffness matrix), which would be a "void," to 100%, which would represent 100% material. This is complicated by the fact that there are two material constituents – an elastic material and a viscoelastic material. This is handled by placing two elements in
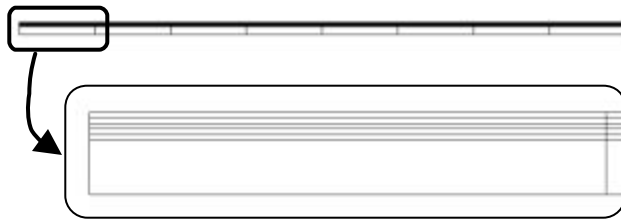
33

FIGURE 3.3 - Symmetric Finite Element Model Used For Topology Optimization

the same location in the constraining layer design space – one that is viscoelastic and one that is elastic. The density (and thus the modulus) of each element is allowed to vary from 0% to 100%, but the total density in each location (the density of the elastic element plus the density of the viscoelastic element) is not allowed to be greater than 100%. Although this is artificial, in that, it is unrealistic to consider manufacturing a structure with these properties, the results of this initial study leads to insight in the optimal constrained layer configuration, and are used to develop a structure that is reasonable to manufacture.

3.5   OPTIMIZATION STATEMENT

The objective of this study is to maximize the system loss factor, measured using the modified modal strain energy method. The design variables are the percentage of material in each element, where 0% represents a void, and 100% represents complete material (elastic or viscoelastic, whichever the case may be). The result is validated by computing the loss factor using the half-power bandwidth method. One constraint on the objective is that the total fraction of each constituent in the constraining layer is fixed. (Technically, this is included as an inequality constraint rather than an equality constraint, but these constraints are virtually always active). For example, in one case, the viscoelastic material is limited to be 20% of the total constraining layer design space, and the elastic material is limited to be another 20%. Furthermore, as mentioned above, the

percentage of viscoelastic material plus the percentage of elastic material must be less than or equal to 100% in each element location. To summarize, the optimization statement may be written:

Minimize: system loss factor

such that:

$$\frac{\sum_{i=1}^{n} d_v^{(i)}}{n} \leq f_v$$

$$\frac{\sum_{i=1}^{n} d_e^{(i)}}{n} \leq f_e$$

$$1 \times 10^{-6} \leq d_v^{(i)} \leq 1 \qquad i = 1,2,\ldots,n$$

$$1 \times 10^{-11} \leq d_e^{(i)} \leq 1 \qquad i = 1,2,\ldots,n$$

$$d_v^{(i)} + d_e^{(i)} \leq 1 \qquad i = 1,2,\ldots,n$$

where:

$d_v^{(i)}$ = the fraction of viscoelastic material in element "i";

$d_e^{(i)}$ = the fraction of elastic material in element "i";

f_v = the total fraction of viscoelastic material;

f_e = the total fraction of elastic material;

n = the number of viscoelastic elements (which is equal to the number of elastic elements).

Thus the material properties for a viscoelastic element are:

$$\rho^{(i)} = d_v^{(i)} \rho_v$$

$$E^{(i)} = d_v^{(i)} E_v$$

and the material properties for an elastic element are:

$$\rho^{(i)} = d_e^{(i)} \rho_e$$

$$E^{(i)} = d_e^{(i)} E_e$$

The lower bounds on the viscoelastic are different than those for the elastic elements because the stiffnesses for these different materials vary by several orders of magnitude.

3.6   OPTIMIZATION PROCESS

One difficulty in the process of optimization is in finding the first bending mode of the structure. As the densities and stiffnesses of the constraining layer elements change, it is possible for new modes to appear locally in the constraining layer. A heuristic method was developed in order to determine which mode of the structure was equivalent to the first mode of the base beam. Initially, it was considered that the mode closest to the natural frequency of the initial structure should be considered as the first mode. However, the process of optimization would tend to produce local constraining layer modes (which were highly damped) that were close to the initial natural frequency,

so another parameter was necessary to use in order to discern which mode was the "first" mode of the beam. The first mode is one where the normalized displacement of the midpoint of the simply supported beam is large, while for the local constraining layer modes, displacements in the constraining layer are much larger than displacements in the base beam. Thus, a criterion for determining which mode to use for computing the loss factor involved adding the inverse of the lowest normalized midpoint displacement for the mode eigenvector with the difference between the natural frequency of the mode with the natural frequency of the structure in the previous optimization step.

A commercial code was used for the optimization, which uses an SQP (sequential quadratic programming) algorithm. For details on the algorithm and the code used (NLPQL), see Schittkowski (1986). Optimization requires a technique for finding the design sensitivities of the objective function (i.e., the gradient of the objective function with respect to the design variables). Finding analytical gradients is an extremely complex task for a problem of this scope, and so numerical gradients are calculated by the finite difference method in the algorithm.

Figure 3.4 shows the Optimization Process Flow Chart. It gives us an idea on how the optimization software in inter-related with the finite element package and the give and take of data is highlighted.
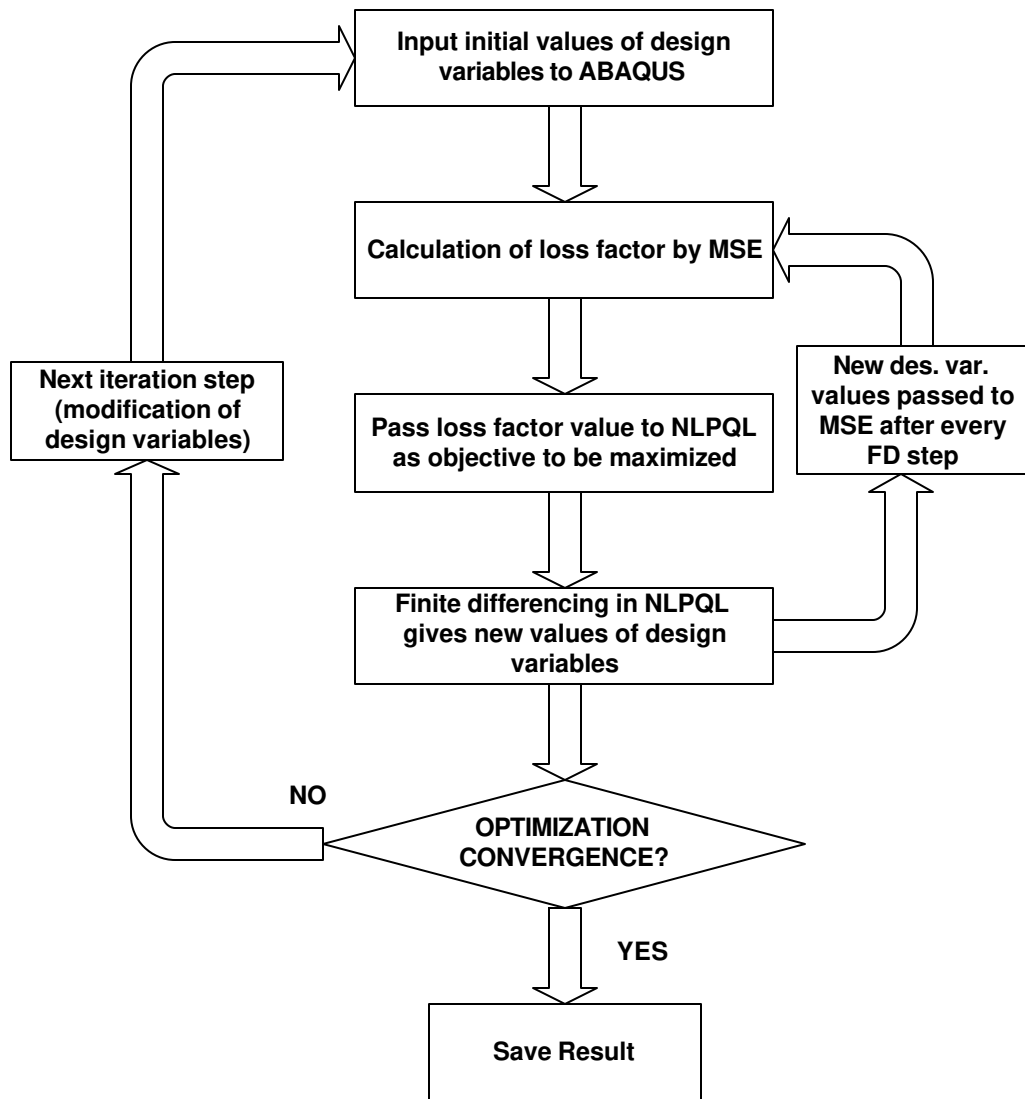
FIGURE 3.4 - Optimization Process Flow Chart

4 RESULTS

In this chapter, the results of all the Parameter Studies are presented. They are divided into the following sections:

1. **Simply Supported Beam**

   - Material Fraction Parameter Study
   - Base Beam Thickness Parameter Study

2. **Cantilever Beam**

   - Free Root Cantilever –Material Fraction Parameter Study
   - Fixed Root Cantilever –Material Fraction Parameter Study

Free Root Cantilever Beam is the one in which the design space, i.e. the constraining layer and the constrained layer is free at both ends and only the base beam is fixed at one end as shown in Figure 4.1.

Fixed Root Cantilever Beam is the one in which the design space, i.e. the constraining layer and the constrained layer is fixed at one end along with the base beam as shown in Figure 4.2.

Prior research (Mantena, et al., 1991) has shown that these two configurations produce substantially different results. Hence, we will separately examine both cases.
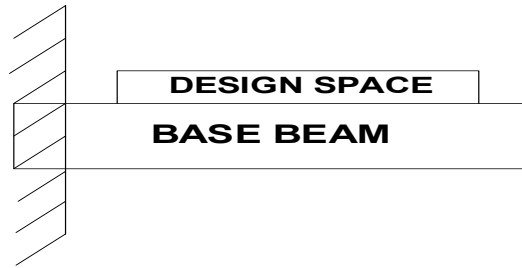
Figure 4.1 - Free Root Cantilever Beam
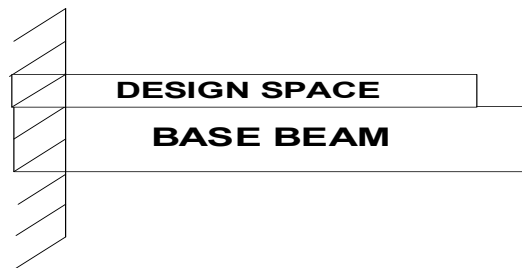
Figure 4.2 - Fixed Root Cantilever Beam

4.1   Material Fraction Parameter Study For Simply Supported Beam

The results of the Parameter Study for a Simply Supported Beam with respect to 'Material Fraction' are shown below. The values for the material fractions used for the study are: 10% to 50% with an increase in 10% for each successive value. A '10% material fraction' means that we have 10% viscoelastic (damping) material and 10% elastic (constraining) material. And since the design space is divided into 5 layers of 8 continuum elements each (it should be noted that only half the beam is modeled because of symmetry), the elements of the first layer are assigned a 'normalized viscoelastic density' of 0.5 and the elements of the second layer are assigned a 'normalized elastic density' of 0.5. (Normalized density refers to the density of each element scaled between 0 and 1, hence a normalized elastic density of 0.5 is hypothetical and it means that the element contains 0.5 times the density of elastic material. Same is the case with viscoelastic material) Hence 0.5 times 8 elements equals 4 full elements which amounts to 10% of the possible material that can occupy the design space. Similarly, 20% material fraction contain one full viscoelastic and elastic layer and 40% material fraction contains 2 full viscoelastic and elastic layers of elements. For the 30% case, the viscoelastic fraction is split into 20%+10% and the elastic fraction is split into 10%+20%. Here, the 10% fractions of both materials combine to form a hypothetical middle layer containing half viscoelastic density and half elastic density. Similarly, the 50% material fractions are split into 20%+20%+10% for each material and the 10% fractions combine to give a middle combination layer. The Initial configurations are shown in Figure 4.3. The heights of the constraining layer elements are exaggerated for clarity purposes.
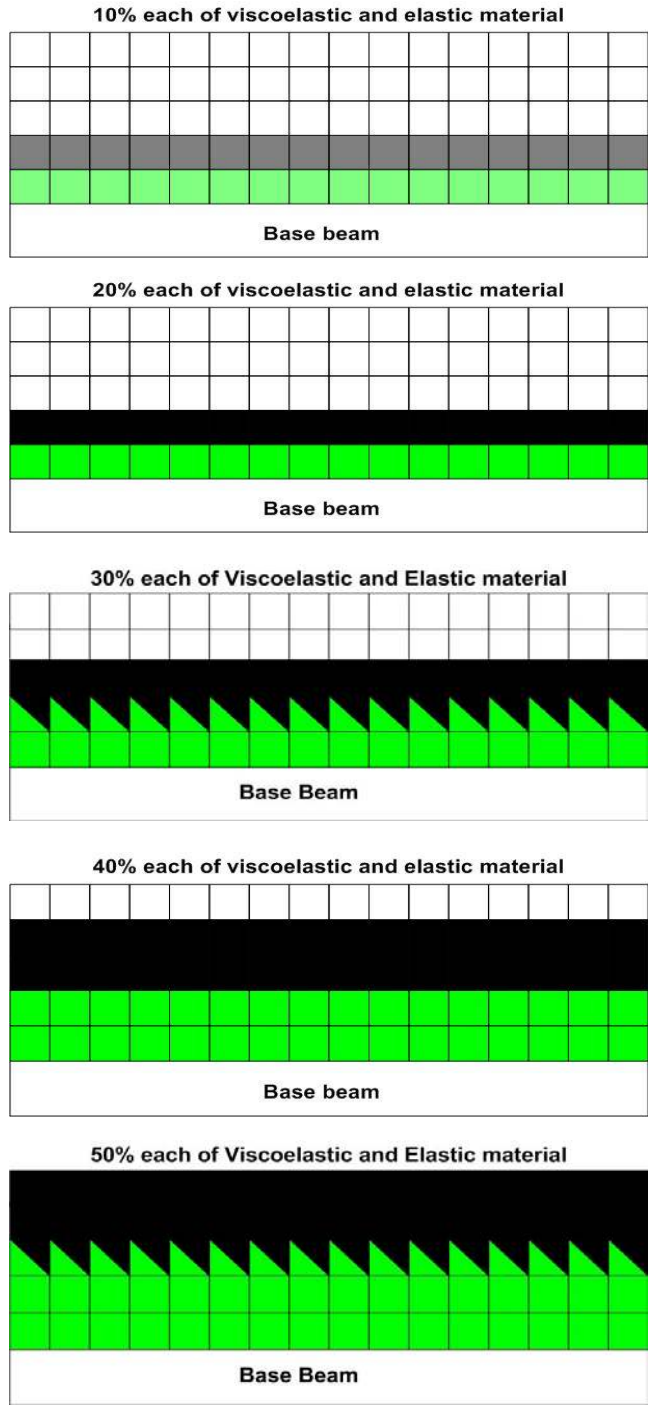
Figure 4.3 – Initial Configurations

Table 4.1 contains the results obtained from optimization of the loss factor for different material fractions using Modified Modal Strain Energy Method (refer page 17). These results are validated, as shown in Table 4.1 itself, by the Half-Power Bandwidth Method from a steady state forced response. We have to accurately model viscoelasticity if we have to use this method.

The increase in the system loss factor is substantial (up to 370%). The final densities of each element for all cases are shown in Figure 4.4. (Both halves of the symmetric model are shown in both Figures). In Figures 4.3 and 4.4, the heights of the constraining layer elements are exaggerated for the sake of clarity; recall that the total height of the constraining layer is only 0.5 millimeters, one-half the height of the base beam. Also the colors of the base beam and the constraining layer are shown to be different even though they are from the same material. This is because the base beam is not part of the design domain, whereas the constraining layer is a part of the design domain along with the viscoelastic material, which is shown in green color.

Each case in Figure 4.4 shows two models for every material fraction, the one on the left indicating the elastic material densities in the design space, and the one on the right indicating the viscoelastic material densities in the design space. This is also done for clarity. In each case, a dark element represents 100% material, and a white element represents a "void." There are some elements, which have densities between 0% to 100%, which can be seen as partly colored or having different shades of the respective colors.

We can observe from the result table that there is not much change in the natural frequency of the structure for every case. Hence, this validates our basic assumption for the modal strain energy method that the material properties are frequency invariant.

44

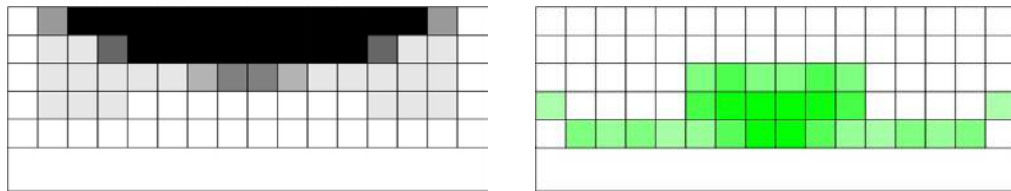**Table 4.1 Results - Material Fraction Parameter Study**

Percentage of material	Initial ω_d (Hz)	Initial η	Final ω_d (Hz)	Final η	% Imp.
10 % by MSE	108.12	0.027	111.41	0.099	270.8
10 % by HPB	109.08	0.0232	114.15	0.1087	369.4
20 % by MSE	112.80	0.046	114.70	0.154	234.4
20 % by HPB	114.48	0.0389	118.58	0.1657	325.9
30 % by MSE	118.66	0.086	117.56	0.188	118.4
30 % by HPB	121.94	0.0756	122.04	0.2018	166.7
40 % by MSE	117.45	0.164	117.76	0.206	25.46
40 % by HPB	122.11	0.1669	122.93	0.2198	31.72
50 % by MSE	121.36	0.211	119.52	0.226	7.0
50 % by HPB	127.21	0.2167	124.64	0.2412	11.3
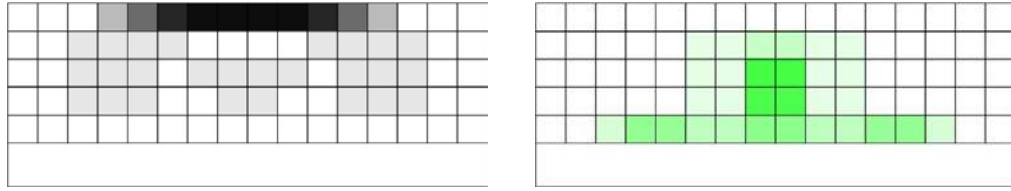
10% Material Fraction
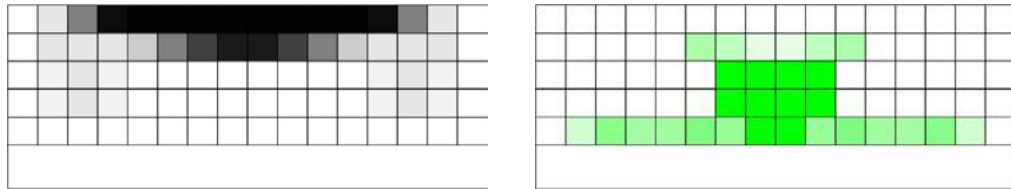
20% Material Fraction

30% Material Fraction
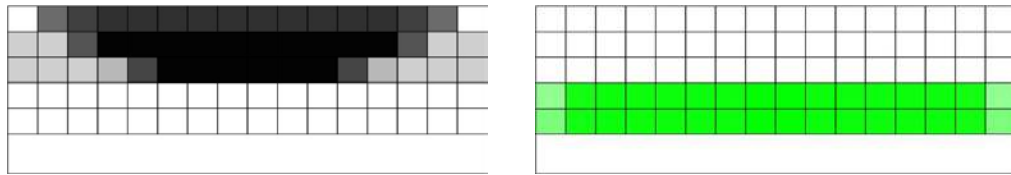
40% Material Fraction
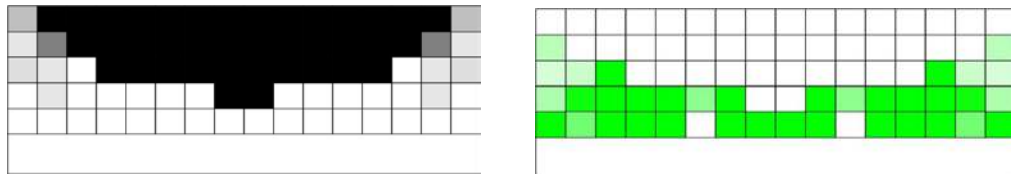
50% Material Fraction

Figure 4.4 – Optimization Results – Material Fraction Parameter Study

The Percentage Improvement in Loss Factor is calculated by:

% Improvement = (final value – initial value) / initial value

From Table 4.1, it is seen that topology optimization produces a significant improvement in the system loss factor. Although the loss factor results for the MSE method are significantly different than those computed from the half-power bandwidth method, since the half power bandwidth method is a more accurate method than modal strain energy method, it is assumed that optimizing using the MSE method is still valid in producing an optimal design that has improved damping characteristics, and this is born out in the optimization results.

Figure 4.5 shows how the initial and optimized loss factors vary with material fractions. Figure 4.6 shows the effectiveness of optimization in maximizing the loss factor. It is clear from Figure 4.4 that for all the cases, the elastic material tends towards being towards the top of the design space and the viscoelastic material tends towards the bottom. What may not be as clear from Figure 4.4 is that the elastic material, in addition to coalescing towards the top of the constraining layer, also develops vertical "columns" which can be seen three elements from the left (or right) end. Although these columns consist of only 1% to 2% elastic material, the stiffness produced is substantial in inducing shearing in the viscoelastic layer, as the stiffness of the elastic material is four orders of magnitude greater than the stiffness of the viscoelastic material.

It can be seen from Figure 4.5 that the MSE method under-predicts the loss factor when compared with the half power bandwidth method, which is the more accurate
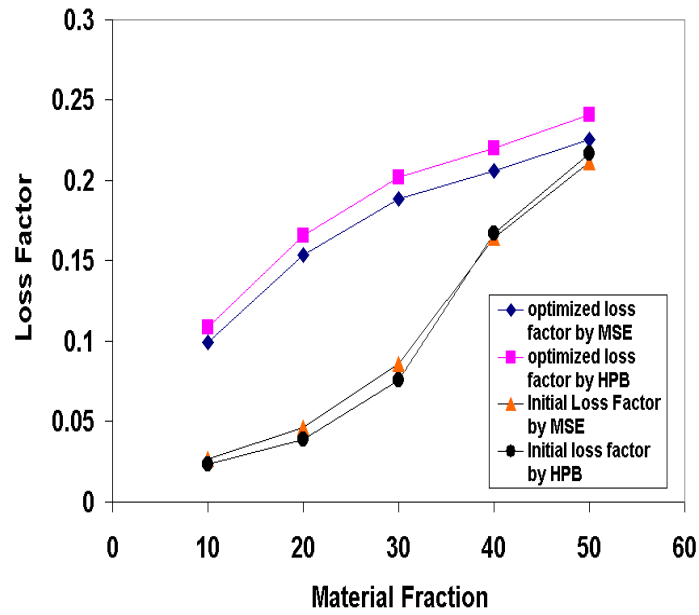
47

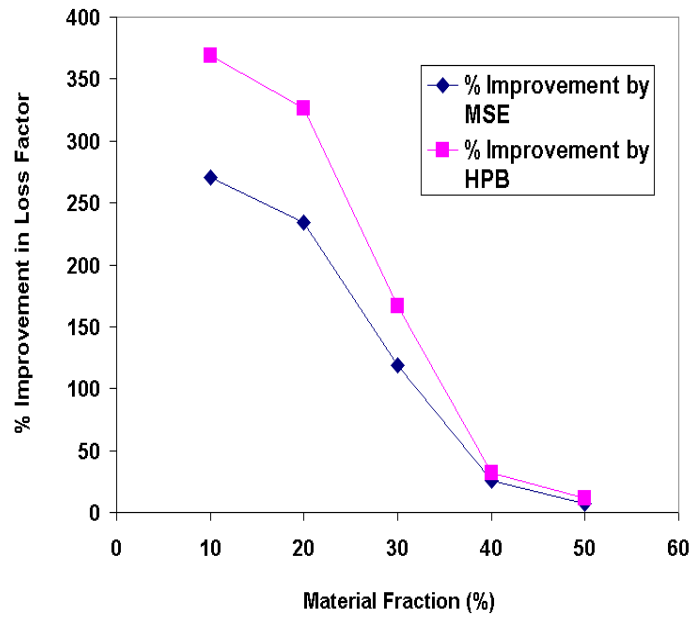**Figure 4.5 – Loss Factor Variation With Material Fraction**

Figure 4.6 – Effectiveness of Optimization

method of the two. But this under-prediction is consistent for all material fractions under consideration and hence gives good confidence in the results obtained. The optimized loss factor increases with increase in material fraction, which is the expected result, since increase in damping material will increase the capacity of the beam to damp out the vibrations and hence result in an increased loss factor.

Figure 4.6 shows significant improvement in loss factors (300%) for smaller material fractions. It can be seen that MSE method again under-predicts the percentage improvement as compared to the half power bandwidth method. Also, this improvement is more pronounced for lower material fractions (10% - 30%) than higher material fractions (40% - 50%). This behavior can be attributed to a 'saturation' reached by the loss factor for that particular damping treatment. Since lower material fractions start with lower loss factors, there is more scope for improvement in such cases than that for higher material fractions. Also, one can observe that as the percentage improvement increases, the under-prediction by MSE method also increases, so that the ratios of the two values of loss factors (from the two different methods) for each material fraction remain nearly the same, thereby showing consistency in the results obtained.

4.2   Base Beam Thickness Parameter Study For Simply Supported Beam

The next set of results is that of the Parametric Study with respect to the 'Base Beam Thickness'. Table 4.2 contains the results obtained from optimization of the loss factor for different base beam thicknesses using Modal Strain Energy Method. This study was carried out for a material fraction of 20% each of damping material and

Table 4.2 – Results - Base Beam Thickness Parameter Study

Base Beam Thickness	Initial ω_d (Hz)	Initial η	Final ω_d (Hz)	Final η	% Imp.
0.5 mm by MSE	66.32	0.0888	64.2	0.2262	154.7
0.5 mm by HPB	68.2	0.0719	67.0	0.2392	232.8
1 mm by MSE	112.8	0.046	114.7	0.1538	234.4
1 mm by HPB	114.5	0.0389	118.6	0.1657	325.9
2 mm by MSE	212.3	0.0217	212.7	0.0634	191.9
2 mm by HPB	213.8	0.0189	216.0	0.0704	272.8
4 mm by MSE	414.9	0.0103	413.2	0.025	143.6
4 mm by HPB	416.3	0.009	416.0	0.0281	211.3
6 mm by MSE	617.9	0.0067	615.1	0.0146	119.4
6 mm by HPB	619.3	0.0059	617.5	0.0161	175.2

constraining material. In this study, different values for the base beam thickness were chosen as listed in Table 4.2, and the loss factor of the resulting structure was optimized. These results are validated, as shown in Table 4.2 itself, by the Half-Power Bandwidth Method from a steady state forced response. Also, the percentage improvement of all results is calculated and shown in Table 4.2 itself. Figure 4.7 shows the variation of the loss factor with base beam thickness. Figure 4.8 shows how effective the optimization process is for different base beam thicknesses by plotting the percentage improvement in loss factor versus the base beam thickness (parameter under study).

From Figure 4.7, it can be seen that the results obtained by the MSE method match their validations done by the half power bandwidth method. Also, as the base beam thickness increases for the same amount of material fraction and beam length, the loss factor decreases proportionately. This is as expected since, as the base beam thickness increases, the strain energy in the elastic beam increases but the volume of damping material remains the same, and hence the loss factor decreases.

From Figure 4.8 we can observe that the percentage improvement in the system loss factor is significantly under-predicted by the MSE method. But since the nature of both the curves is the same, it gives good confidence in the results obtained. Even though the MSE method under-predicts the improvement in the loss factor, it shows a very significant improvement (above 100%) for all values of the parameter considered for study. There is a maximum improvement for a certain base beam thickness (close to 1 mm) and then it decreases uniformly for the remaining values.
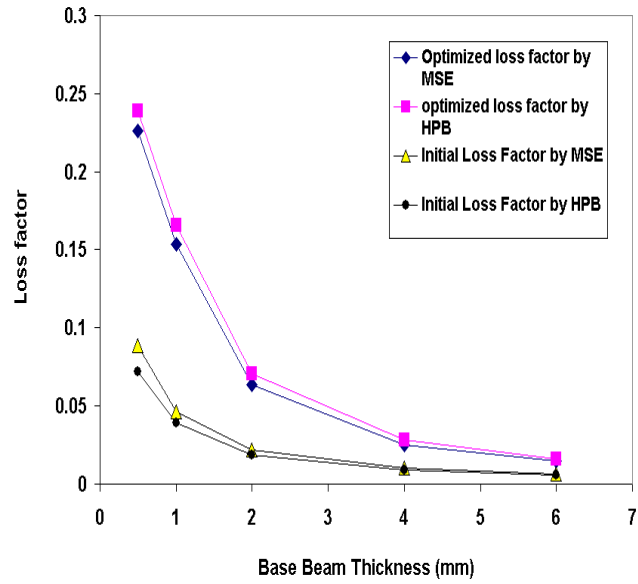
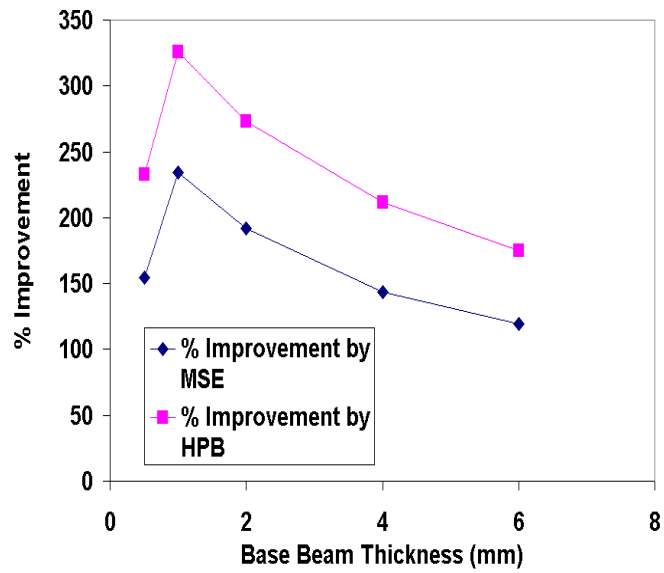**Figure 4.7 – Loss Factor Variation With Base Beam Thickness**

Figure 4.8 – Effectiveness Of Optimization

Figure 4.9 shows the optimal shapes for the base beam parameter study results with elastic elements on the left and viscoelastic elements on the right. It can be seen that different topologies emerge for the different base beam heights. Although some general principles for design are clear (viscoelastic material has highest density toward the bottom of the design space in every case, elastic material tends toward the top of the design space in every case, "column-like" elastic structures emerge in every case), it appears that the optimal topologies have some different characteristics for different base beam heights as well. This can be noted from the fact that for the 0.5 mm, 4 mm and 6 mm base beam thickness, the elastic constraining material tends to form a double-layered structure, joined by two columns in between them. Further study is required in order to determine the significance of these different characteristics in the damping layer design.

4.3   Manufacturable Configurations For Material Fraction Parameter Study

The common difficulty with topology optimization is that the resulting structures are often extremely difficult to manufacture because of partial densities at many locations, as well as dual densities at a few element locations, as is the case here. So, the topology optimization results were used to interpret a design that would be reasonable to manufacture, where every element is either 100% damping material, 100% elastic material, or empty. To arrive at a reasonable manufacturable solution, a two-stage process was followed:
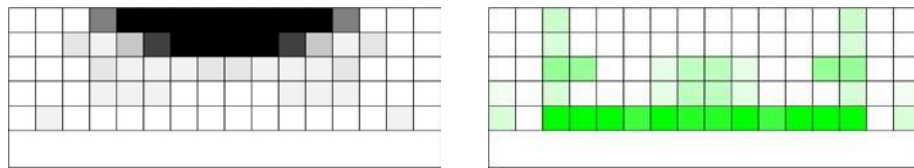
1.   Initially, every element from the optimal result that consisted of more than 1% material was made to be 100% elastic or 100% viscoelastic. The problem with this
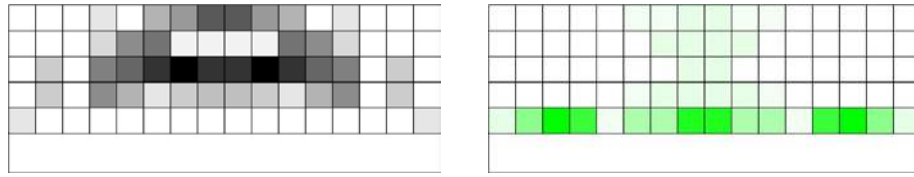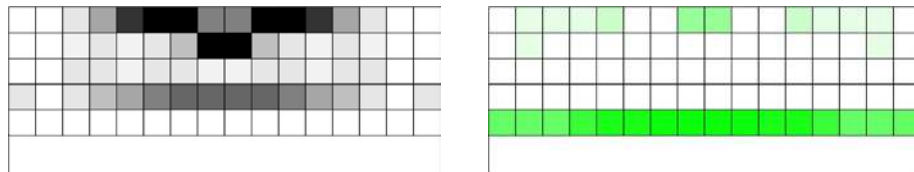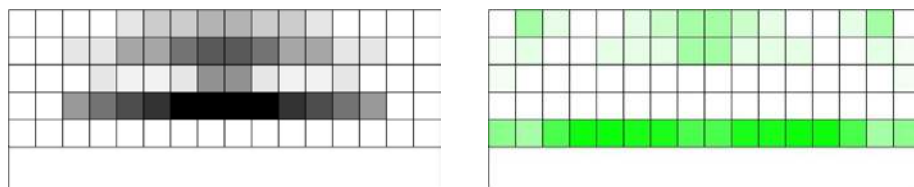
0.5 mm base beam
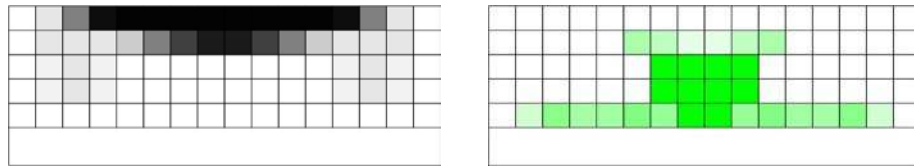
1 mm base beam

2 mm base beam

**4 mm base beam**

6 mm base beam

Figure 4.9 – Optimization Results - Base Beam Thickness Parameter Study

stage is that most of the times, we ended up with a configuration that has more material volume than the initial configuration and hence a comparison between the two configurations could not be made. So, further interpretation was required in order to demonstrate the validity of the optimization result, comparing equivalent volumes of materials. This step was done only for the 20% case.

2. In this stage, the material fractions of the interpreted configurations were matched with their respective initial configurations for comparison purposes. The damping elements to be retained were determined by removing those that had the lowest stresses. In all other cases, this was done intuitively.

Based on this two-stage process, the interpreted configurations for the material fraction parameter study for a simply supported beam are shown in Figure 4.10.

It is clear from the optimal solutions of all cases (Figure 4.6) that the elastic constraining material tends towards being towards the top of the design space and the viscoelastic material tends towards the bottom. What may not be as clear from Figure 4.6 is that the elastic material, in addition to coalescing towards the top of the constraining layer, also develops vertical "columns" which can be seen three elements from the left (or right) end. Although these columns consist of only 1% to 2% elastic material, the stiffness produced is substantial in inducing shearing in the viscoelastic layer, as the stiffness of the elastic material is four orders of magnitude greater than the stiffness of the viscoelastic material. These vertical columns play an important role in interpreting the shapes of structure, which are reasonable to manufacture (Figure 4.10). Hence, as you
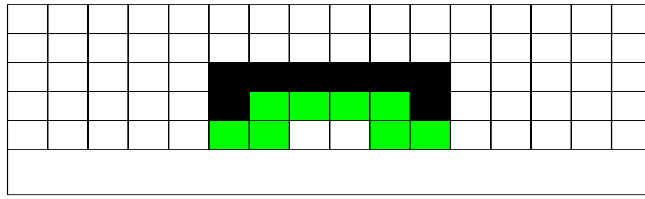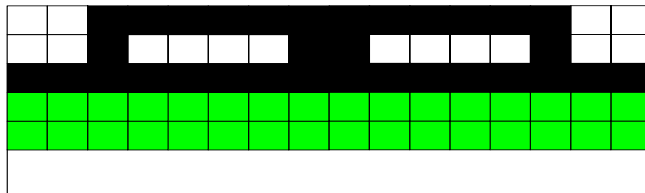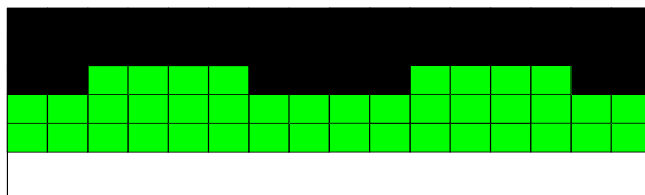
10% material fraction
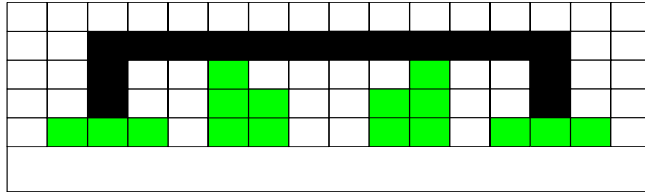
20% material fraction

30% material fraction

40% material fraction

50% material fraction

Figure 4.10 – Interpreted Configurations - Material Fraction Parameter Study

can see in Figure 4.10 that almost all interpreted shapes have these vertical columns to induce shearing in the viscoelastic layer, which dissipates more energy, thereby increasing the loss factor.

Table 4.3 gives the loss factors for the interpreted shapes in Figure 4.10 calculated by half-power bandwidth method. From Table 4.3, it is clear that the improvements in loss factor are lower than those obtained for the optimal shapes. But even then, these improvements are substantial enough when compared to the initial configurations. From the Table 4.3, we can observe that the nature of the improvement curve for the interpreted shapes is the same as that for the optimal configurations except for the case of 10% material fraction., where the interpreted shape has too low an improvement than the optimal solution for the same case. The % improvement is higher for lower values of material fraction, since the material has more space to move in the design domain (eg.10%, 20%, 30%) whereas it is much lower for the 40% and 50% case.

4.4 Manufacturable Configurations For Base Beam Thickness Parameter Study

Since the 20% material fraction case gives consistently higher loss factor values for the optimal configuration as well as the interpreted configuration, we choose this to be the material fraction for all the cases of the Base Beam Thickness Parameter Study. Figure 4.11 shows the manufacturable solutions for the five cases under study.

Table 4.4 gives the loss factors for the interpreted shapes in Figure 4.11 calculated by half-power bandwidth method. From Table 4.4, it is clear that the improvements in loss factor are lower than those obtained for the optimal shapes. But even then, these

57

**Table 4.3 – Results - Interpreted Shapes For Material Fraction Parameter Study**

Material Fraction	Initial η	Final η	Interpreted ω_d (Hz)	Interpreted η	% Imp. Of Interpreted Shape	% Imp. Of Optimal Shape
10% HPB	0.023	0.109	102.516	0.0560	141.4	369.4
20% HPB	0.039	0.166	114.8	0.1123	189	325.9
30% HPB	0.076	0.202	121.83	0.1520	101	166.7
40% HPB	0.167	0.22	123.68	0.1909	14.4	31.72
50% HPB	0.217	0.241	123.68	0.2205	2	11.3

Table 4.4 – Results - Interpreted Shapes for Base Beam Thickness Parameter Study
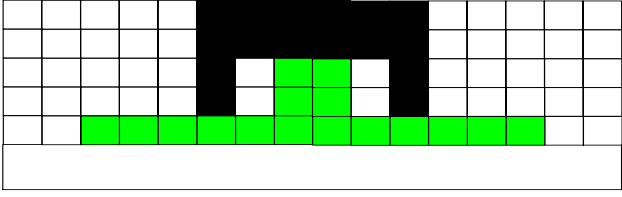
| Material Fraction	Initial η	Final η	Interpreted ω_d (Hz)	Interpreted η	% Imp. Interpreted Shape	% Imp. Optimal Shape
0.5 mm HPB	0.0719	0.2392	62.96	0.2079	189.15	232.8
1 mm HPB	0.0389	0.1657	114.8	0.1123	189	325.9
2 mm HPB	0.0189	0.0704	199.8	0.0406	114.8	272.8
4 mm HPB	0.009	0.0281	407.85	0.025	177.8	211.3
6 mm HPB	0.0059	0.0161	613.3	0.0122	106.8	175.2
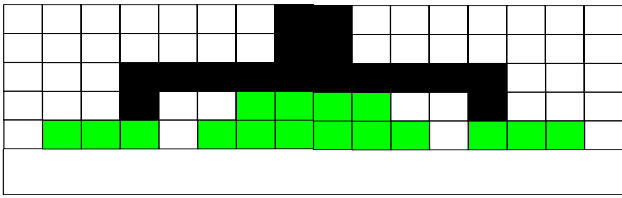
0.5 mm base beam thickness
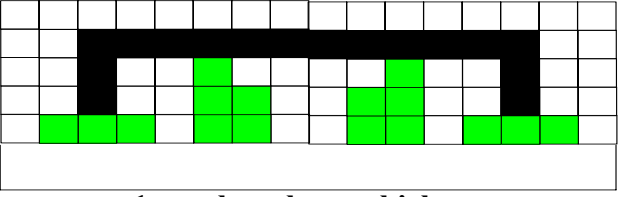
1 mm base beam thickness

2 mm base beam thickness
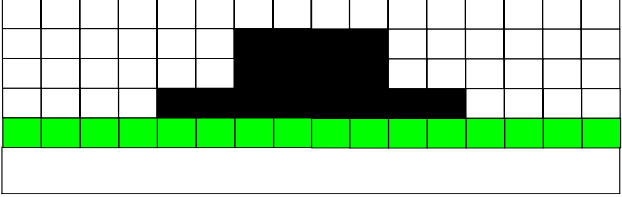
4 mm base beam thickness
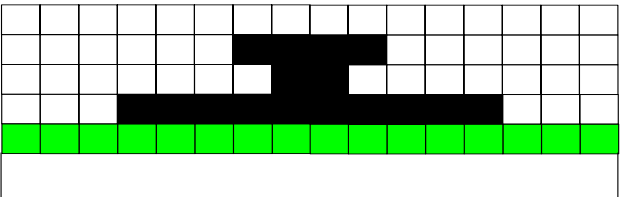
6 mm base beam thickness

Figure 4.11 – Interpreted Configurations - Base Beam Thickness Parameter Study

improvements are substantial enough when compared to the initial configurations. From the loss factor calculations, it is observed that the loss factor value decreases as the base beam thickness increases, which is consistent with the optimal solutions obtained.

In most of the optimal solutions for the cases above, the elastic material tends to form a double layer structure joined by columns. This characteristic of the optimal shape has been retained in the interpreted shape.

4.5   Material Fraction Parameter Study For Fixed Root Cantilever Beam

The results of the Parameter Study for a Fixed Root Cantilever Beam with respect to 'Material Fraction' are shown below. The values for the material fractions used for the study are: 10% to 50% with an increase in 10% for each successive value. A '10% material fraction' means that we have 10% viscoelastic (damping) material and 10% elastic (constraining) material. In this study, the complete beam is modeled as opposed to the simply supported beam where only half the beam was modeled due to symmetry.

And since the design space is divided into 5 layers of 16 continuum elements each, the elements of the first layer are assigned a 'normalized viscoelastic density' of 0.5 and the elements of the second layer are assigned a 'normalized elastic density' of 0.5. (Normalized density refers to the density of each element scaled between 0 and 1, hence a normalized elastic density of 0.5 is hypothetical and it means that the element contains 0.5 times the density of elastic material. Same is the case with viscoelastic material) Hence 0.5 times 16 elements equals 8 full elements which amounts to 10% of the possible material that can occupy the design space. Similarly, 20% and 40% have one and

two full layers of elements respectively, while the 30% and 50% have a middle layer, which is half elastic and half viscoelastic.

Table 4.5 contains the results obtained from optimization of the loss factor for different material fractions using Modal Strain Energy Method. These results are validated, as shown in Table 4.5 itself, by the Half-Power Bandwidth Method from a steady state forced response.

The increase in the system loss factor is substantial. The final densities of each element for all cases are shown in Figure 4.12. In Figure 4.12, the heights of the constraining layer elements are exaggerated for the sake of clarity; recall that the total height of the constraining layer is only 0.5 millimeters, one-half the height of the base beam. Each case in Figure 4.12 shows two models, one indicating the elastic material densities in the design space, and one indicating the viscoelastic material densities. This is also done for clarity. In each case, a dark element represents 100% material, and a white element represents a "void."

From Table 4.5, it is seen that topology optimization produces a significant improvement in the system loss factor. Although the loss factor results for the MSE method are significantly different than those computed from the half-power bandwidth method, and since the half power bandwidth method is a more accurate method than modal strain energy method, it is assumed that optimizing using the MSE method is still valid in producing an optimal design that has somewhat improved damping characteristics, and this is born out in the optimization results.

Figure 4.13 shows how the initial and optimized loss factors vary with material fractions. Figure 4.14 shows the effectiveness of optimization in maximizing the loss

Table 4.5 – Results - Material Fraction Parameter Study For A Fixed Root
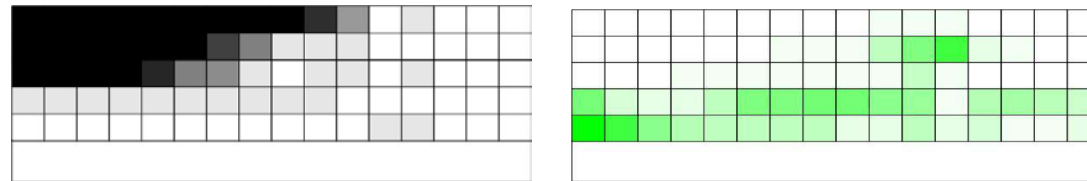
Cantilever Beam

| Percentage of material	Initial ω_d (Hz)	Initial η	Final ω_d (Hz)	Final η	% Imp.
10 % by MSE	38.39	0.0111	42.1	0.1107	897
10 % by HPB	39.04	0.0091	43.24	0.1214	1234
20 % by MSE	40.64	0.0181	44.28	0.1488	722
20 % by HPB	40.89	0.0146	45.66	0.1618	1008
30 % by MSE	43.26	0.0344	46.55	0.1913	456
30 % by HPB	43.74	0.0283	48.46	0.2045	622
40 % by MSE	45.0	0.0819	45.25	0.1937	136.5
40 % by HPB	46.16	0.0713	46.96	0.2069	190
50 % by MSE	47.48	0.1086	45.67	0.2818	159.5
50 % by HPB	49.0	0.0953	48.76	0.2174	128
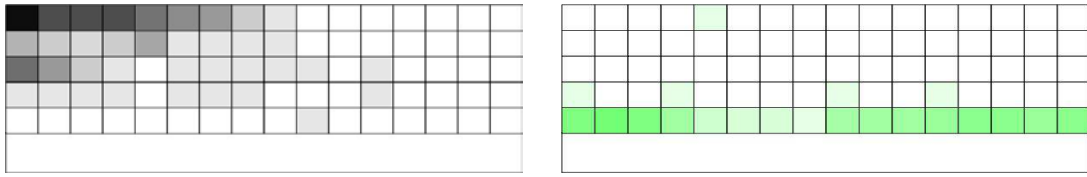
10% material fraction - fixed root cantilever
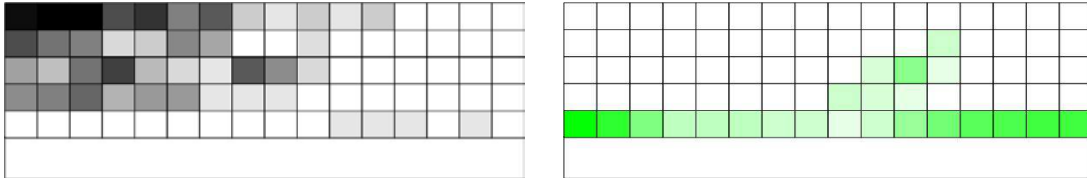
20% material fraction - fixed root cantilever

30% material fraction - fixed root cantilever
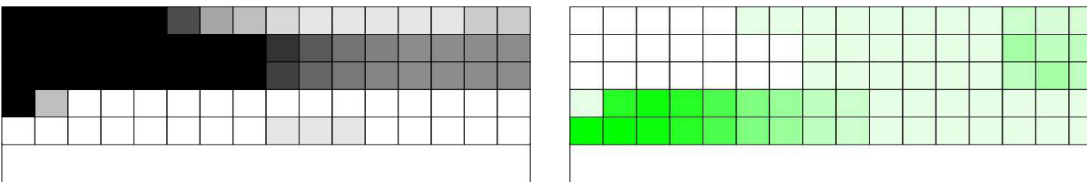
40% material fraction - fixed root cantilever
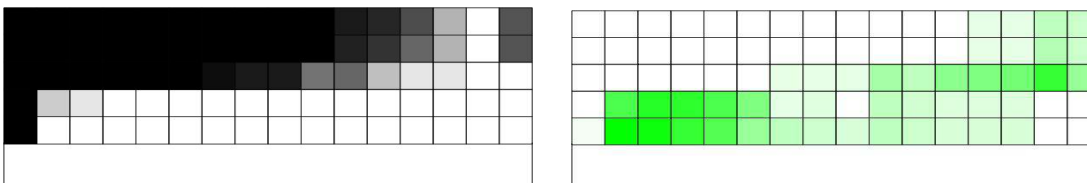
50% material fraction - fixed root cantilever

Figure 4.12 – Optimization Results – Material Fraction Parameter Study For A

Fixed Root Cantilever Beam

factor. It can be seen from Figure 4.13 that the MSE method under-predicts the loss factor when compared with the half power bandwidth method, which is the more accurate method of the two. But this under-prediction is consistent for all material fractions under consideration except for the 50% case and hence gives good confidence in the results obtained. The over-prediction of MSE in this case may be attributed to the basic assumption of the MSE method that it is an accurate method for low damping values and starts to break down at higher values of damping since the mode shapes of the undamped system no longer remain similar to those of the damped system. The optimized loss factor increases with increase in material fraction, which is the expected result, since increase in damping material will increase the capacity of the beam to damp out the vibrations and hence result in an increased loss factor. Another significant observation is that the MSE method over-predicts the initial loss factors for all cases but under-predicts the optimal loss factors. Hence, the % Improvement for MSE is lower than that of HPB, which is the more accurate method of the two.

Figure 4.14 shows significant improvement in loss factors (1000%) for smaller material fractions. It can be seen that MSE method again under-predicts the percentage improvement as compared to the half power bandwidth method. Also, this improvement is more pronounced for lower material fractions (10% - 30%) than higher material fractions (40% - 50%). This behavior can be attributed to a 'saturation' reached by the loss factor for that particular damping treatment. Since lower material fractions start with lower loss factors, there is more scope for improvement in such cases than that for higher material fractions. Also, one can observe that as the percentage improvement increases, the under-prediction by MSE method also increases, so that the ratios of the two values of
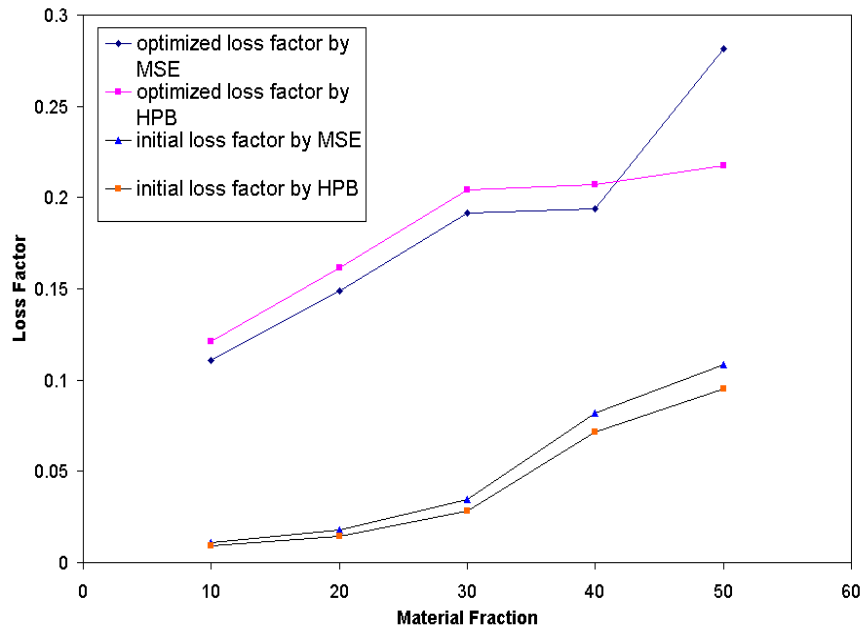
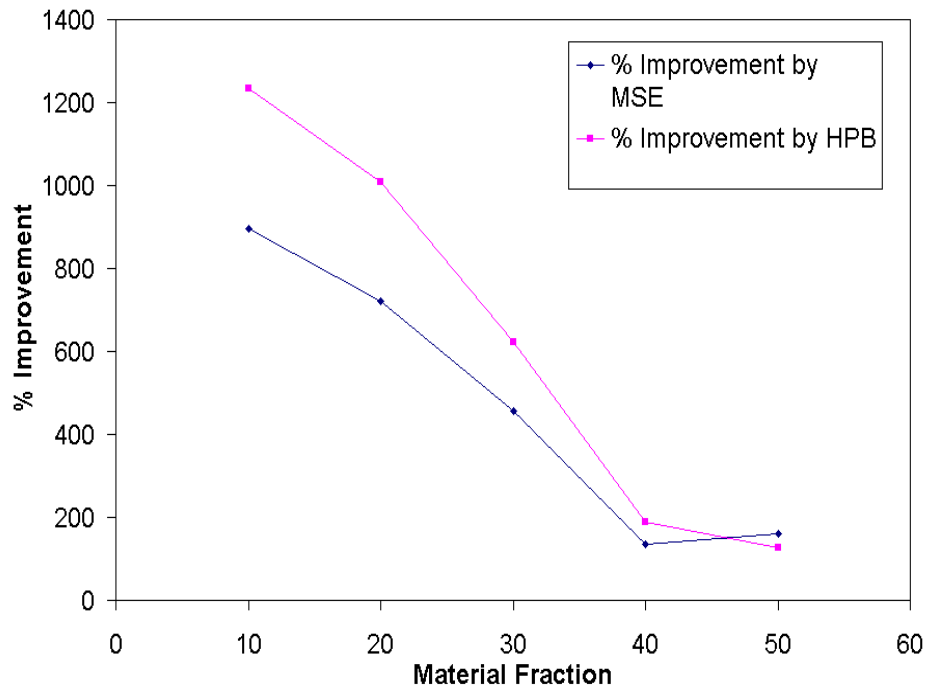**Figure 4.13 – Loss Factor Variation With Material Fraction**

Figure 4.14 – Effectiveness Of Optimization

loss factors (from the two different methods) for each material fraction remain nearly the same, thereby showing consistency in the results obtained.

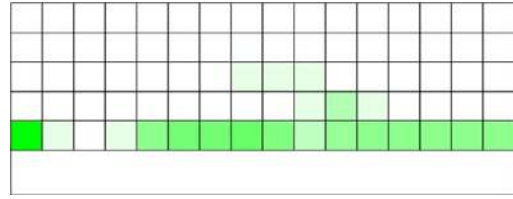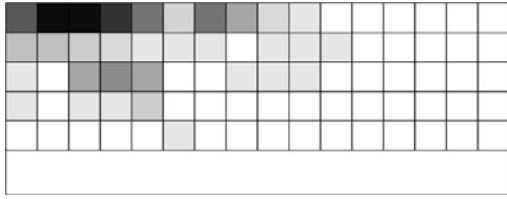## 4.6   Material Fraction Parameter Study For Free Root Cantilever Beam

The results of the Parameter Study for a Fixed Root Cantilever Beam with respect to 'Material Fraction' are shown below. The values for the material fractions used for the study are: 10% to 30% with an increase in 10% for each successive value. A '10% material fraction' means that we have 10% viscoelastic (damping) material and 10% elastic (constraining) material. In this study, the complete beam is modeled as opposed to the simply supported beam where only half the beam was modeled due to symmetry. Only 3 different material fraction cases are documented here, since the optimization process was not able to converge on to a certain optimum for the 40% and 50% cases. This reveals another facet of the optimization process that even though it might seem obvious to find a certain optimum for a given problem (since just a boundary condition has been changed here), it may not necessarily be the case.

The remaining characteristics of this study are similar to those of the Free Root Cantilever Beam Study. Hence, one may refer to that study for any clarifications. Table 4.6 contains the results obtained from optimization of the loss factor for different material fractions using Modal Strain Energy Method. These results are validated, as shown in Table 4.6 itself, by the Half-Power Bandwidth Method from a steady state forced response. The increase in the system loss factor is substantial. The final densities of each element for all cases are shown in Figure 4.15.

67

Table 4.6 – Results - Material Fraction Parameter Study For A Free Root

Cantilever Beam

Percentage of material	Initial ω_d (Hz)	Initial η	Final ω_d (Hz)	Final η	% Imp.
10 % by MSE	37.23	0.0257	40.63	0.0913	255
10 % by HPB	37.48	0.0274	41.48	0.1039	279
20 % by MSE	37.69	0.0445	41.73	0.1333	200
20 % by HPB	38.11	0.0467	42.78	0.1530	227
30 % by MSE	38.13	0.0703	42.29	0.140	99
30 % by HPB	38.75	0.0751	43.41	0.1595	112

10% material fraction - free root cantilever
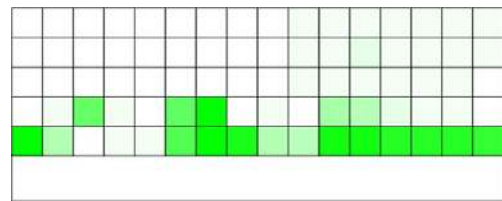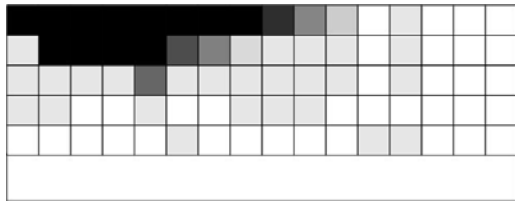
20% material fraction - free root cantilever
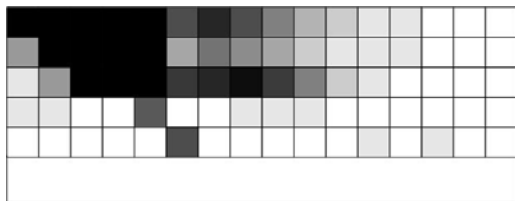
30% material fraction - free root cantilever

Figure 4.15 – Optimization Results – Material Fraction Parameter Study For A

Free Root Cantilever Beam

Figure 4.16 shows how the initial and optimized loss factors vary with material fractions. Figure 4.17 shows the effectiveness of optimization in maximizing the loss factor. It can be seen from Figure 4.16 that the MSE method under-predicts the loss factor when compared with the half power bandwidth method, which is the more accurate method of the two. The optimized loss factor increases with increase in material fraction, which is the expected result, since increase in damping material will increase the capacity of the beam to damp out the vibrations and hence result in an increased loss factor.

Figure 4.17 shows significant improvement in loss factors (250%) for smaller material fractions. It can be seen that MSE method again under-predicts the percentage improvement as compared to the half power bandwidth method. Also, this improvement is more pronounced for lower material fractions than higher material fractions. This behavior can be attributed to a 'saturation' reached by the loss factor for that particular damping treatment. Since lower material fractions start with lower loss factors, there is more scope for improvement in such cases than that for higher material fractions. Also, one can observe that as the percentage improvement increases, the under-prediction by MSE method also increases, so that the ratios of the two values of loss factors (from the two different methods) for each material fraction remain nearly the same, thereby showing consistency in the results obtained.

Another very significant observation is that though the initial loss factor values for fixed root cantilever beam are lower than their respective loss factor values for free root cantilever beam, they end up having higher values after the optimization process than their free root counterparts. Hence they have huge % improvements (of the order of 1000%) as compared to the free root values (of the order of 250%).
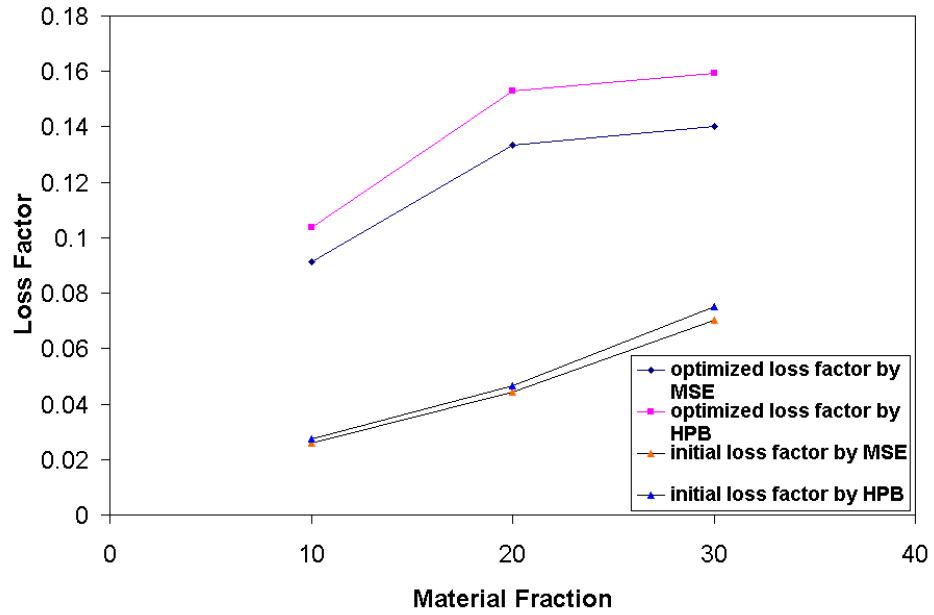
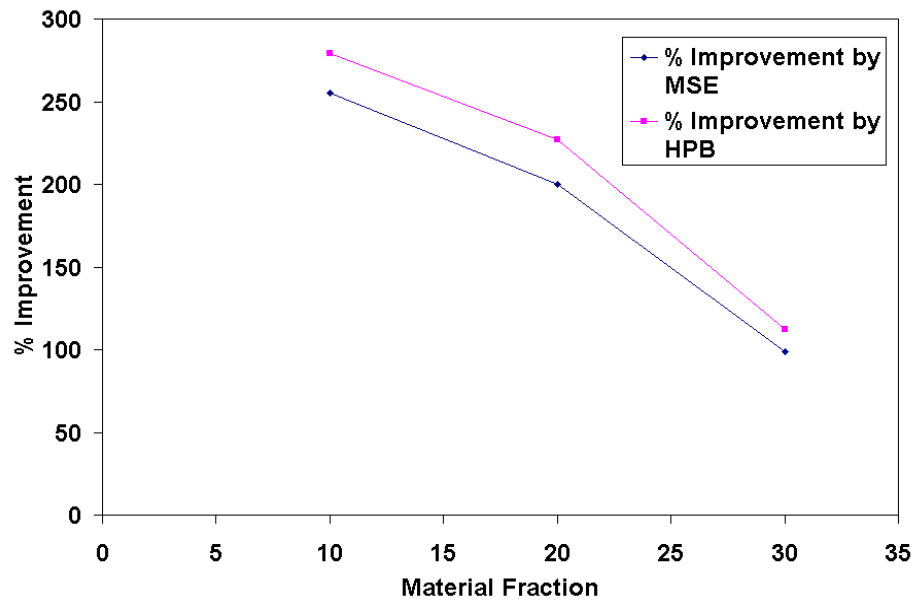**Figure 4.16 – Loss Factor Variation With Material Fraction**


Figure 4.17 – Effectiveness Of Optimization

"Hence, for higher damping, using optimal configurations, a fixed root cantilever is a better option than a free root cantilever, but using initial configurations, a free root cantilever is the better option than a fixed root cantilever beam."

4.7   Manufacturable Configurations For Material Fraction – Fixed Root Cantilever Beam Parameter Study


Figure 4.18 shows the manufacturable solutions for the different cases under study. Table 4.7 gives the loss factors for the interpreted shapes in Figure 4.18 calculated by half-power bandwidth method. From Table 4.7, it is clear that the improvements in loss factor are lower than those obtained for the optimal shapes. But even then, these improvements are substantial enough when compared to the initial configurations. From the loss factor calculations, it is observed that the loss factor value increases as the material fraction increases, which is as expected since with more damping material, the structure is able to damp out more vibrations and hence has a higher loss factor.

In all of the optimal solutions for the cases above, the elastic material tends to accumulate at the fixed end of the structure. This characteristic of the optimal shape has been retained in the interpreted shape. Also, it was observed that more layers of elastic material at the fixed end produce a higher loss factor. The viscoelastic material, for some reason, tends to accumulate at the free end of the structure in the optimal configurations. One needs to dig deeper into the damping mechanism followed to find out why it does so.

The percentage improvement in loss factors of the interpreted shapes shows a similar trend to those of the respective optimal shapes, thereby giving confidence in the
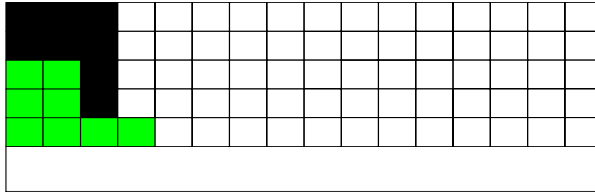
72

10% material fraction
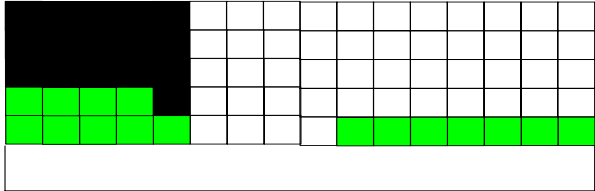
20% material fraction
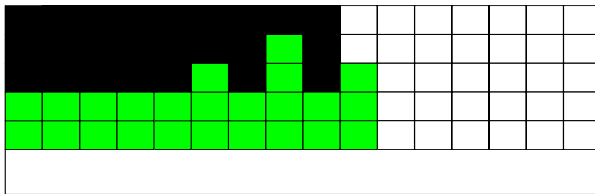
30% material fraction
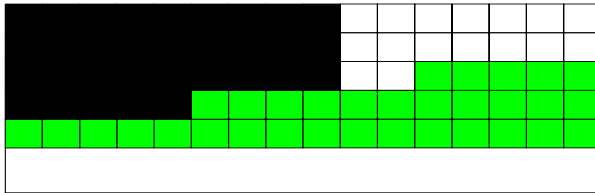
40% material fraction

Figure 4.18 – Interpreted Configurations - Material Fraction Parameter Study

Table 4.7 – Results - Interpreted Shapes For Fixed Root Cantilever Beam Material

Fraction Parameter Study

Material Fraction	Initial η	Final η	Interpreted ω_d (Hz)	Interpreted η	% Imp. Interpreted Shape	% Imp. Optimal Shape
10% HPB	0.0091	0.1214	39.58	0.0802	781	1234
20% HPB	0.0146	0.1618	41.58	0.1401	860	1008
30% HPB	0.0283	0.2045	50.65	0.1701	501	622
40% HPB	0.0713	0.2069	50.35	0.1726	142	190

results obtained. As the material fraction increases, the percentage improvement reduces as expected because the material gets lesser and lesser space to move in the design domain.

5   CONCLUSION AND FUTURE WORK

The topology of a constrained damping layer was optimized for maximizing the damping loss factor for different boundary conditions viz. simply supported beam and cantilever beam, and substantial improvements (up to 1200%) were found by the redistribution of the material constituents compared to a standard constraining layer. The finite element calculation has been linked with the commercial optimization code NLPQL and a number of parameter studies have been conducted. More insight on how the system responds to change in certain parameters was obtained by carrying out these parameter studies. The parameters that were varied were the material fraction and the base beam thickness. The percentage improvement graphs give us a better understanding on where to trade off between amount of material to be used and the loss factor required. Additionally, it was determined that there is an optimal base beam thickness in order to obtain maximum improvement in the system loss factor from topology optimization.

The loss factor was calculated successfully in most of the cases by the Modal Strain Energy Method, which is an approximate method. This was done to reduce the computational time drastically. Novel designs for the constrained damping layer emerged from the optimization process that show promise for improved damping performance. Previous research showed that a design could be interpreted from these optimization results that still shows a substantial increase in damping without substantial additional manufacturing or material cost. Hence, a few interpreted shapes based on the tendency of the material to move in a particular region in the design space were shown corresponding

to their optimal solutions already obtained from the optimization process, for example, in case of the cantilever beams, the material tends to get collected in the areas of high bending moment i.e. near the fixed end of the beam or in case of the base beam thickness study, the elastic constraining layer tends to form a double layered structure joined by columns in between. These tendencies of the material are retained while interpreting the shapes that are reasonable to manufacture. A constraint put on these interpreted shapes was that the material fraction to be used in these shapes should be the same as the initial configuration on which these shaped are based.

There is a lot of future scope for this research. Firstly, experimental verification of the results obtained computationally can be done. To this effect, a few initial steps have been taken. The Experimental Setup along with the necessary hardware and software has been put up. A few preliminary experiments have been performed which give good confidence in the approach followed. Once the required custom fabricated samples are obtained, the experimental process would get going. Another very significant and important feature to be looked at is the Homogenization process. Homogenized material elements can be used instead of the two material elements. This would improve the results dramatically.

It is furthermore possible to implement a penalty function in the optimization setup, which forces all elements to be either 100% material or to be void. This would enable the optimization software itself to determine a more manufacturable solution. A parameter study, as done in this study, can be conducted to get a deeper understanding of this area. Future studies could easily be extended by studying other geometries, boundary conditions or initial optimization points. It is possible to give a non-uniform density distribution as initial point of the optimization, and to examine the results of these

optimizations. We can use any other start point too. This will ensure that the result obtained is the optimum over a wider range.

After completion of this study, an optimization including piezoelectric and viscoelastic material could be conducted, to get topologies such as an active constrained layer damping (ACLD) structure (Lumsdaine 2001). The goal of this optimization would be to determine the best topology of these two materials, which leads to the best topology for active constrained layer damping.

REFERENCES

REFERENCES

ANSYS Theory manual for Revision 5.5

Bendsoe, M. P., Optimization of Structural Topology, Shape, and Material, pg. 10, Springer-Verlag, 1995.

Bendsoe, M. P., and Kikuchi, N., "Generating Optimal Topologies in Structural Design using a Homogenization Method," Computer Methods in Applied Mechanics and Engineering, Vol. 71, No. 2, pp. 197-224, 1988.

Di Taranto, R. A., "Theory of the vibratory bending for elastic and viscoelastic layered finite length beams," Journal of Applied Mechanics, Vol. 32 (Trans ASME Series E87, 881)

Ewins, D. J, Modal Testing: Theory, Practice and Application, 2nd Edition, Research Studies Press, Ltd., Hertfordshire, England, 2000.

Hajela, P., and Lin, C-Y., "Optimal Design of Viscoelastically Damped Beam Structures", Applied Mechanics Review, Vol. 44, No. 11, Part 2, pp. S96-S106, 1991.

Hsu, Y.-C. and Shen, I. Y., "Constrained Layer Damping Treatments for Microstructures," Journal of Vibration and Acoustics, Vol. 124. No. 4, pp. 612-616, 2002.

Hwang, S. J., Gibson R. F., and Singh, J., "Decomposition of Coupling Effects on Damping of Laminated Composites Under Flexural Vibration", Composites Science and Technology, Vol. 43, pp. 159-169, 1992.

Johnson, C. D., and Kienholz, D. A., "Finite Element Prediction of Damping in Structures with Constrained Viscoelastic Layers," <u>AIAA Journal</u>, Vol. 20, No. 9, pp. 1284 - 1290, 1981.

Kerwin, E. M., Jr. "Damping of flexural waves by a constrained viscoelastic layer," <u>Journal of Acoustic Society of America</u>, Vol. 31, No. 7, 1959

Lall, A. K., Nakra, B. C., and Asnani, N. T., "Optimum Design of Viscoelastically Damped Sandwich Panels", <u>Engineering Optimization</u>, Vol. 6, pp. 197-205, 1983.

Lam, M. J., Inman, D. J., and Saunders, W. R., "Hybrid Damping Models using the Golla-Hughes-McTavish Method with Internally Balanced Motion Reduction as Output Feedback," <u>Smart Materials and Structures</u>, Vol. 9, No. 3, pp. 362-371, 2000.

Lekszycki, T. and Olhoff, N., "Optimal Design of Viscoelastic Structures Under Forced Steady-State Vibration," <u>The Journal of Structural Mechanics</u>, Vol. 9, pp. 363-387, 1981.

Lesieutre, G. A. and Mingori, D. L., "Finite-Element Modeling of Frequency-Dependent Material Damping Using Augmenting Thermodynamic Fields," <u>Journal of Guidance Control and Dynamics</u>, Vol. 13, No. 6, pp. 1040-1050, 1990.

Liao, W. H., and Wang, K. W., "A New Active Constrained Layer Configuration with Enhance Boundary Actions," <u>Smart Materials and Structures</u>, Vol. 5, No. 5, pp. 638-648, 1996

Lifshitz, J. M., and Leibowitz, M., "Optimal Sandwich Beam Design for Maximum Viscoelastic Damping", <u>International Journal of Solids and Structures</u>, Vol. 23, No. 7, pp. 1027 - 1034, 1987.

Lin, T.-C. and Scott, R. A., "Shape Optimization of Damping Layers," Proceedings of the 58th Shock and Vibration Symposium, Huntsville, Alabama, Vol. 1, pp. 395-409, 1987.

Liu, Q., and Chattopadhyay, A., "Improved Helicopter Aeromechanical Stability Analysis Using Segmented Constrained Layer Damping and Hybrid Optimization," Journal of Intelligent Material Systems and Structures, Vol. 11, No. 6, pp. 492-500, June 2000.

Liu, Y, and Wang, K. W., "A Non-Dimensional Parametric Study of Enhanced Active Constrained Layer Damping Treatments," Journal of Sound and Vibration, Vol. 223, No. 4, pp. 611-644, 1999.

Lumsdaine, A. and Scott, R. A., "Shape Optimization of Unconstrained Beam and Plate Damping Layers", Proceedings of the American Society of Mechanical Engineers 15th Biennial Conference on Mechanical Vibration and Noise, Boston, MA, 1995.

Lumsdaine, A. and Scott, R. A., "Optimal Design of Constrained Plate Damping Layers Using Continuum Finite Elements", Proceedings of the International Symposium on Advanced Materials for Vibro-Acoustic Application, 1996 American Society of Mechanical Engineers International Mechanical Engineering Congress and Exposition, pp. 159-168, Atlanta, GA, 1996.

Lumsdaine, A. and Scott, R. A., "Shape Optimization of Unconstrained Viscoelastic Layers Using Continuum Finite Elements," Journal of Sound and Vibration, Vol. 216, No. 1, pp. 29-52, 1998.

Lumsdaine, A., "Topological Optimization of Constrained Damping Layer Treatments," Proceedings of the ASME International Mechanical Engineering Congress

and Exposition, 2002 ASME International Mechanical Engineering Congress and Exposition, New Orleans, LA, IMECE2002-39021, 2002.

Lundén, R., "Optimum Distribution of Additive Damping of Vibrating Beams," Journal of Sound and Vibration, Vol. 66, pp. 25-37, 1979.

Lundén, R., "Optimum Distribution of Additive Damping of Vibrating Frames," Journal of Sound and Vibration, Vol. 72, pp. 391-402, 1980.

Mantena, Raju P., Gibsor, R. F., Hwang, S. J., " Optimal Constrained Viscoelastic Tape Lengths for Maximizing Damping in Laminated Composites", AIAA Journal Vol. 29, pp. 1678-1685, 1991.

Mead, D. J., Markus, S., " The Forced Vibration of a Three-Layer, Damped Sandwich Beam with Arbitrary Boundary Conditions", 1969, Journal of Sound and Vibration, Vol. 10 (2), pp. 163-175

Miles, R. N., Reinhall, P. G., " An Analytical Model for the vibration of laminated beams including the effects of both shear and thickness deformation in the adhesive layer", Journal Of Vibration, Acoustics, Stress and Reliability in Design, Vol. 108, pp. 56-64, 1986

Moran, B., and Knauss, W. G., "Crack-Tip Stress and Deformation Fields in Strain-Softening Nonlinearly Viscoelastic Materials", Journal of Applied Mechanics, Vol. 59, pp. 95 - 101, 1992.

Nakra, B. C., "Vibration Control with Viscoelastic Materials," The Shock and Vibration Digest, Vol. 8, pp. 3-12, 1976.

Nakra, B. C., "Vibration Control with Viscoelastic Materials--II," <u>The Shock and Vibration Digest</u>, Vol. 13, pp. 17-20, 1981.

Nakra, B. C., "Vibration Control with Viscoelastic Materials--III," <u>The Shock and Vibration Digest</u>, Vol. 16, pp. 17-22, 1984.

Nashif, A.D., Jones, D. I. G., Henderson, J. P., "Vibration Damping", <u>John Wiley & Sons</u>, New York, 1985

Oberst, H. and Frankenfeld, K., "Uber die Damfug der Biegeshwingungen dunner Bleche dunch fest habtende Belage's," <u>Acustica</u>, Vol. 2, pp. 181-194, 1952.

Plunkett, R. and Lee, C. T., "Length Optimization for Constrained Viscoelastic Layer Damping", <u>The Journal of the Acoustical Society of America</u>, Vol. 48, No. 1, pp. 150-161, 1970.

Rao, M. D., "Recent Applications of Viscoelastic Damping for Noise Control in Automobiles and Commercial Airplanes," <u>Journal of Sound and Vibration</u>, Vol. 262, pp. 457-474, 2003.

Rao, D. K., "Frequency and Loss Factors of Sandwich Beams Under Various Boundary Conditions", <u>Journal of Mechanical Engineering Science</u>, Vol. 20, No. 5, pp. 271-282, 1978.

Rigbi, Z., "The Value of Poisson's Ratio of Viscoelastic Materials", <u>Applied Polymer Symposia</u>, Vol. 5, pp. 1 - 8, 1967.

Ross, D., Ungar, E. E., and Kerwin, E. M., "Damping of Plate Flexural Vibrations by Means of Viscoelastic Laminae," Section 3, American Society of Mechanical Engineers Monograph on Structural Damping, 1959.

Roy, P. K., and Ganesan, N., "Dynamic Studies on Plates with Unconstrained Layer Treatment," Computers and Structures, Vol. 49, pp. 473-480, 1993.

Roy, P. K., and Ganesan, N., "Dynamic Studies on Beams with Unconstrained Layer Treatment," Journal of Sound and Vibration, Vol. 195, pp. 417-427, 1996.

Rozvany, G. I. N., Zhou, M., and Birker, T., "Generalized Shape Optimization Without Homogenization," Structural Optimization, Vol. 4, pp. 250-252, 1992.

Schittkowski, K., "NLPQL: A FORTRAN Subroutine for Solving Constrained Non-linear Programming Problems," ed. C. L. Monma, Annals of Operations Research, Vol. 5, pp. 485 - 500, 1986.

Sigmund, O., and Torquato, S., "Design of Materials with Extreme Thermal Expansion using a Three-Phase Topology Optimization Method," Journal of the Mechanics and Physics of Solids, Vol. 45, No. 6, 1997.

Sisemore, C. L. and Darvennes, C. M., "Transverse Vibration of Elastic-Viscoelastic-Elastic Sandwich Beams: Compression—Experimental and Analytical Study," Journal of Sound and Vibration, Vol. 252, No. 1, pp. 155-167, 2002.

Ungar, E. E., and Kerwin, E. M., "Loss Factors of Viscoelastic Systems in Terms of Energy Concpets," Journal of the Acoustical Society of America, Vol. 34, pp. 954-957, July 1962.

Van der Sluis, O., Vosbeek, P. H. J., Schreurs, P. J. G., and Meijer, H. E. H., "Homogenization of Heterogeneous Polymers," International Journal of Solids and Structures, Vol 36, pp. 3193-3214, 1999.

Xu, Y., Chen, D., " Finite Element Modeling for the Flexural Vibration of Damped Sandwich Beams Considering Complex Modulus of the Adhesive Layer", <u>Proceedings of SPIE</u>, Vol.3989, Damping and Isolation, pp. 121-129, Newport Beach, California, 2000.

Xu, Y., Liu, Y., and Wang, B., "Revised Modal Strain Energy Method for Finite Element Analysis of Viscoelastic Damping Treated Structures," <u>Proceedings of the SPIE 9th Annual Symposium on Smart Structures and Materials</u>, Vol. 4697, pp. 35-42, San Diego, CA, 2002.

Yang, R. J., and Chuang, C. H., "Optimal Topology Design Using Linear Programming," <u>Computers and Structures</u>, Vol. 52, No. 2, pp. 265-275, 1994.

Yi, Y.-M., Park, S.-H., and Youn, S.-K., "Design of Microstructures of Viscoelastic Composites for Optimal Damping Characteristics," <u>International Journal of Solids and Structures</u>, Vol. 37, pp. 4791-4810, 2000.

Yildiz, A. and Stevens, K., "Optimum Thickness Distribution of Unconstrained Viscoelastic Damping Layer Treatments for Plates," <u>Journal of Sound and Vibration</u>, Vol. 103, pp. 183-199, 1985.

VITA

Rohan Vinay Pai was born on December 1st 1979 in a town called Pune, situated near the west coast of Inida. In olden days, Pune was known as 'The Oxford of the East' for its University and the standard of education. His did his schooling from Loyola High School, one of the better schools in his town. He obtained his Bachelor of Engineering (B.E.) Degree from Pune University in Mechanical Engineering in 2001. He obtained his Master of Science Degree from the University of Tennessee, Knoxville in December 2003 and is currently pursuing a Doctoral Degree from the same University in Mechanical Engineering with a concentration in Vibration Damping. He has been fully funded throughout his Masters and Doctorate.